DNA Repair Protein APE1 Degrades Dysfunctional Abasic mRNA in Mitochondria Affecting Oxidative Phosphorylation

Arianna Barchiesi [1], Veronica Bazzani [1], Agata Jabczynska [2], Lukasz S. Borowski [2,3], Silke Oeljeklaus [4], Bettina Warscheid [4,5], Agnieszka Chacinska [6,7], Roman J. Szczesny [2] and Carlo Vascotto [1,6]*

*1 - **Department of Medicine,** University of Udine, 33100 Udine, Italy*
*2 - **Institute of Biochemistry and Biophysics,** Polish Academy of Sciences, Pawinskiego 5A, 02-106 Warsaw, Poland*
*3 - **Faculty of Biology,** Institute of Genetics and Biotechnology, University of Warsaw, Pawinskiego 5A, 02-106 Warsaw, Poland*
*4 - **Biochemistry and Functional Proteomics,** Institute of Biology II, Faculty of Biology, University of Freiburg, 79104 Freiburg, Germany*
*5 - **Signalling Research Centres BIOSS and CIBSS,** University of Freiburg, Germany*
*6 - **Laboratory of Mitochondrial Biogenesis,** Centre of New Technologies, University of Warsaw, 02-097 Warsaw, Poland*
*7 - **ReMedy International Research Agenda Unit,** Centre of New Technologies, University of Warsaw, 02-097 Warsaw, Poland*

Correspondence to Carlo Vascotto:*University of Udine, DAME, P.le Kolbe 4, 33100 Udine, Italy. *carlo.vascotto@uniud.it (C. Vascotto)*
https://doi.org/10.1016/j.jmb.2021.167125
Edited by Philip C. Bevilacqua

Abstract

APE1 is a multifunctional protein which plays a central role in the maintenance of nuclear and mitochondrial genomes repairing DNA lesions caused by oxidative and alkylating agents. In addition, it works as a redox signaling protein regulating gene expression by interacting with many transcriptional factors. Apart from these canonical activities, recent studies have shown that APE1 is also enzymatically active on RNA molecules. The present study unveils for the first time a new role of the mitochondrial form of APE1 protein in the metabolism of RNA in mitochondria. Our data demonstrate that APE1 is associated with mitochondrial messenger RNA and exerts endoribonuclease activity on abasic sites. Loss of APE1 results in the accumulation of damaged mitochondrial mRNA species, determining impairment in protein translation and reduced expression of mitochondrial-encoded proteins, finally leading to less efficient mitochondrial respiration. Altogether, our data demonstrate that APE1 plays an active role in the degradation of the mitochondrial mRNA and has a profound impact on mitochondrial well-being.

Introduction

Human apurinic/apyrimidinic endonuclease 1 (APE1) is a protein with multifunctional roles that was first described almost thirty years ago for its endonuclease activity on apurinic DNA[1] and as a redox activator of the transcription factor AP-1.[2] Further studies have demonstrated how, through a redox mechanism, APE1 activates several other transcriptional factors, including NF-κB,[3] the tumor-suppressor protein p53,[4] HIF-1α,[5] STAT3,[6] Egr-1,[7] Pax8,[8] and a few others. Concerning its enzymatic activity on DNA, APE1 exhibits not only class II apurinic/apyrimidinic (AP) site incision activity, which makes it a key component of the DNA base excision repair (BER) pathway,[9] but it also possesses the ability to excise 3′-damages.[10] In addition, APE1 has been shown to exhibit 3′ to 5′

exonuclease activity, which is, however, poorly processive and $\geq$ 100-fold less efficient compared to its AP endonuclease activity.[11]

DNA and RNA molecules differ in their chemistry and structure, and specific and distinct enzymes are involved in DNA repair and RNA metabolism. However, evidence emerging over the last few years has indicated that certain DNA repair proteins are also involved in the RNA quality control processes, identifying damaged, chemically modified or oxidized RNA, which may lead to ribosomal malfunctioning, error-prone protein translation, and—as a final consequence—failed protein synthesis.[12] In this regard, the first evidence for APE1 enzymatic action on RNA *in vitro* was the identification of its RNase H-like activity on a DNA/RNA duplex[13] and the capacity to cleave an AP site-containing ssRNA.[14] Next, Lee and colleagues identified APE1 as the endoribonuclease responsible for cleaving a specific coding region of the c-*myc* mRNA, demonstrating for the first time the ability of APE1 to affect mRNA half-life and therefore supporting its role in RNA metabolism.[15] In the last decade, Tell and colleagues thoroughly investigated the uncanonical role of APE1 in RNA biology. In 2009, an interactomic study led to the identification and characterization of several novel APE1 partners which, unexpectedly, included a number of proteins involved in ribosome biogenesis and RNA processing.[16] More recently, our knowledge about the enzymatic activity of APE1 toward RNA was extended as a result of its demonstrated ability to recognize and efficiently process an abasic or oxidized ribonucleoside 5′-monophosphate (rNMP) erroneously incorporated, and then damaged, into a DNA strand.[17] Finally, in 2017 the Tell group unveiled the association of APE1 with the miRNA processing complex DROSHA and its active role in the processing of miR-221/222.[18] All these independent studies clearly showed that, apart from being an essential DNA repair protein, the nuclear form of APE1 is also enzymatically active on RNA molecules.

APE1 is not present only within the nuclear compartment. Its minor fraction is translocated through the TOM pore into the mitochondrial inner membrane space (IMS),[19] where it becomes the substrate of the mitochondrial intermembrane space assembly (MIA) pathway,[20] to be finally translocated through the TIM23/PAM complex into the mitochondrial matrix.[21] Importantly, it has been demonstrated that APE1 translocates into mitochondria in response to oxidative stress, increasing the mitochondrial DNA (mtDNA) repair rate and therefore promoting cell survival.[21,22] Mitochondria are an important endogenous source of reactive oxygen species (ROS) production, which are generated as by-products of the normal metabolism.[23] The mtDNA has been shown to accumulate high levels of 8-hydroxy-2′-deoxyguanosine, being the product of guanine hydroxylation at carbon 8, which is a mutagenic lesion.[24] ROS-induced oxidative lesions and alkylated bases in DNA are repaired via BER, the major DNA repair mechanism acting in mitochondria, and APE1, which acts as a key component of the pathway.[25] However, RNA is also subjected to oxidative damage, and 8-hydroxyguanosine is the only oxidized base characterized so far in RNA,[26] which indicates that this common oxidative modification to DNA occurs in RNA as well. Oxidative damage can alter RNA structure and function and interfere with the interaction between RNA and other cellular molecules.[27] Moreover, oxidation of mRNA leads to reduced translation efficiency and abnormal protein production[28] and causes ribosome dysfunction.[29] Despite many efforts, information about the processes involved in degradation of RNA in human mitochondria is still scanty. While RNA helicase SUV3 and ribonuclease PNPase were shown to be essential for mitochondrial RNA (mtRNA) degradation, the role of other proteins in mtRNA decay remains to be established.[30–32] In particular, to our knowledge, nothing is known about the mechanism responsible for degradation of damaged mitochondrial messenger RNAs (mt-mRNAs).

Data presented in this manuscript unveil a new function of the mitochondrial form of the DNA repair protein APE1, proving for the first time its active role in the degradation of damaged mt-mRNAs and its strong impact on mitochondrial well-being.

Results

APE1 binds mitochondrial mRNA

In this study we used a HeLa-based cell model developed in our laboratory[33] where APE1 expression could be downregulated by inducible expression of APE1-specific siRNA (shRNA) or a control scramble sequence (Scr) and at the same time a siRNA-resistant ectopic FLAG-tagged APE1 form could be expressed ($APE1^{WT}$). Western blot analysis confirmed that mitochondrial APE1 expression is efficiently reduced and that ectopic FLAG-tagged $APE1^{WT}$ localizes into the mitochondrial compartment (Figure 1(A)). Loss of APE1 expression determines a plethora of effects, among which are mitochondrial membrane depolarization and induction of mitochondrial-mediated apoptosis.[34] One of the results of mitochondrial stress is the increase of mtDNA content to limit the possible detrimental effects of ROS on DNA and, as a consequence, on the mitochondrial protein synthesis.[35] To prove that silencing of APE1 is a stress-causing condition for mitochondria in our cell model, we measured the mtDNA content before and after APE1 knockdown in HeLa cells. As shown in Figure 1(B), APE1 depletion leads to an increase of the amount of mtDNA copy number in comparison to the control $APE1^{WT}$ clone. Next, we evaluated the mitochondrial transcription by measuring

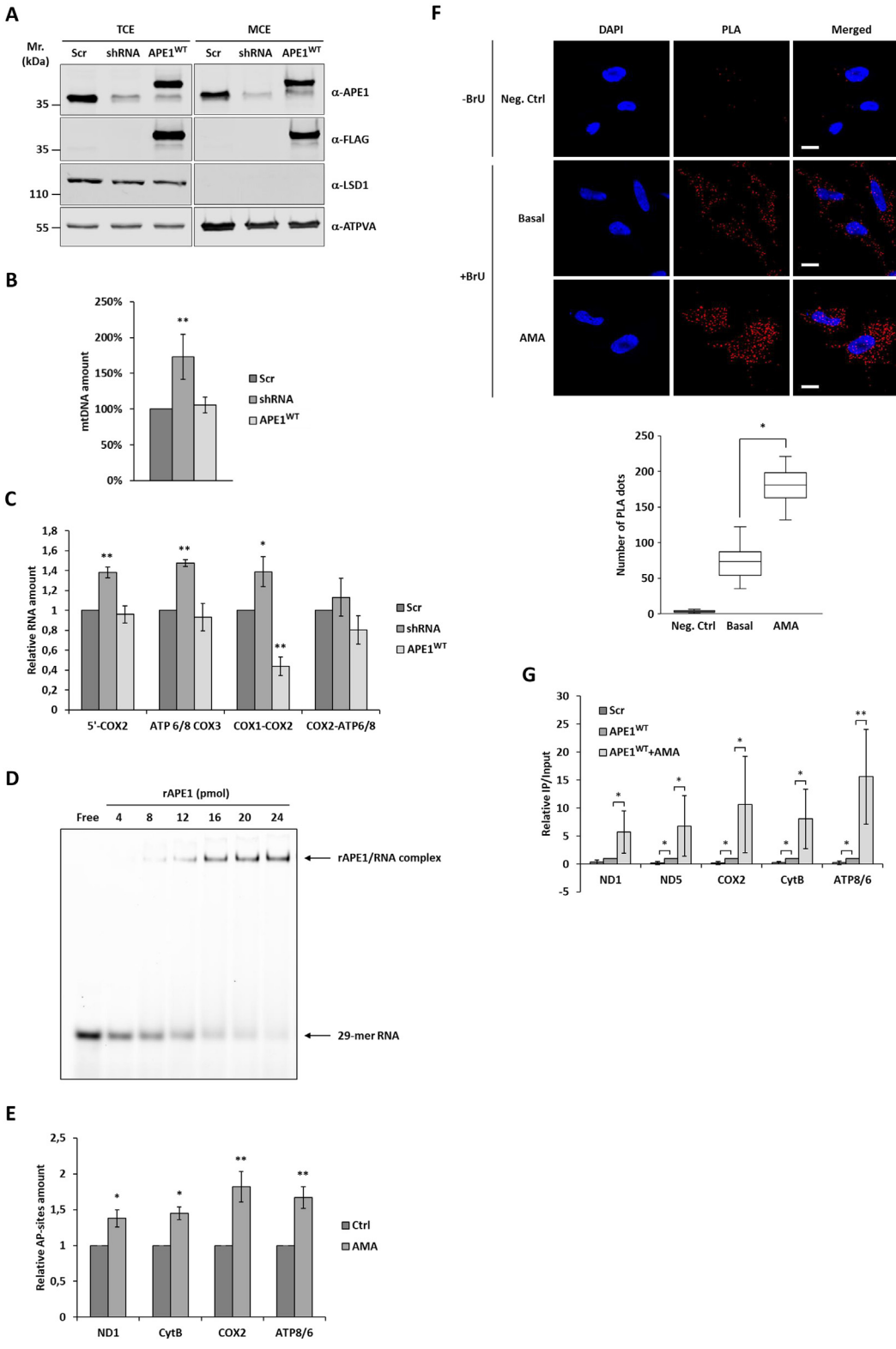

the levels of precursor polycistronic RNA (5′-COX2, ATP8/6-COX3, COX1-COX2, COX2-ATP8/6). As for the mtDNA levels, all unprocessed transcripts were also upregulated in APE1 shRNA cells and rescued in the APE1^{WT} clone, confirming the biological relevance of mitochondrial APE1 and the reliability of our study model (Figure 1(C)). In the case of COX1-COX2, expression levels were even lower in the APE1^{WT} clone than in the control, but we have no explanation for this. As first step to

evaluate the ability of APE1 to bind mitochondrial mRNA, we performed electrophoretic mobility shift assay (EMSA) analysis using recombinant APE1 (rAPE1) (Supplementary Figure S1) and a 29-mer ribonucleotide with the sequence of mitochondrial COX2 mRNA as probe. After increasing the concentration of rAPE1, a retarded band constituted by the rAPE1/RNA complex was visible (Figure 1 (D)).

Like DNA, RNA can also undergo oxidative damage; the prevalent oxidized base in RNA is 8-hydroxyguanosine (8-OHG), which could be released, leaving AP-sites[36] that are targets of APE1. We treated HeLa cells with Antimycin A (AMA), an inhibitor of the mitochondrial electron transport chain complex III, which inhibition specifically induces mitochondrial oxidative stress.[21,37] Isolated RNA was derivatized by treatment with an aldehyde-reactive probe (ARP), followed by purification with magnetic beads. Precipitated AP-RNA and total RNA were subjected to qRT-PCR for ND1, CytB, COX2, and ATP8/6. All mt-mRNAs showed more damage after AMA treatment (Figure 1(E)).

To ascertain if APE1 also binds RNA molecules *in vivo*, and to evaluate if the binding is increased when RNA is damaged, we performed a proximity ligation assay (PLA) analysis. Newly synthetized RNA was labeled with bromouridine (BrU) by 30-minute incubation of HeLa cells with 2.5 mM of BrU[38] (Supplementary Figure S2); unlabeled cells (Bru-) were used as PLA control and AMA-treated cells were also included in the analysis. This assay allowed us to monitor interactions of endogenous proteins directly or with a nucleic acid, as well as protein post-translational modification with high specificity and sensitivity.[39] The presence of dots in the metabolically labeled cells (BrU +) confirmed the interaction between APE1 and RNA (Figure 1 (F)). Moreover, to evaluate whether the binding of APE1 increased upon oxidative stress, cells labeled with BrU were treated with AMA for 30 minutes at the final concentration of 25 μM.[21] The analysis has established that APE1 constitutively binds to RNA (70 ± 21 PLA dots/cell) and that this binding is significantly enhanced by the induction of mitochondrial oxidative stress (179 ± 24 PLA dots/cell). Interestingly, the large majority of PLA signals are extra-nuclear, raising the possibility that APE1 could bind and exert endoribonuclease activity on abasic RNA (AP-RNA) in mitochondria. Because co-localization experiments with MitoTracker were not conclusive and considering that PLA analysis provided evidence only of the proximity between APE1 and extranuclear RNA without proving their direct binding, we decided to use an alternative approach to demonstrate that APE1 binds mitochondrial mRNA. Total cell lysates from scramble and APE1^{WT} HeLa clones described in Figure 1 (A) were incubated with anti-FLAG magnetic beads to immunoprecipitate APE1 and then eluates were analyzed for the presence of mtDNA (ND1, ND5, COX2, CytB and ATP8/6) and nDNA (NDUFA1, UQCRC2, COXB2, ATPVA) encoded mRNAs. The relative IP amount with respect to the input (total RNA) has been calculated and data have been reported with respect to the wild-type clone, whose value was settled to 1. As visible in Figure 1(G), APE1 binds mitochondrial mRNAs, and in accordance with the PLA analysis, treatment with AMA significantly increases the amount of mRNAs co-immunoprecipitated with APE1. With respect to nuclear-encoded mRNAs, our analysis showed complete absence of amplification for all analyzed mRNA species both under basal conditions and after treatment with AMA, indicating that these

Figure 1. APE1 binds mitochondrial messenger RNA. (A) Western blot analysis of total cell extract (TCE) and mitochondrial extract (MCE) of cell clones used in this study. Control (Scr), APE1 shRNA (shRNA), and APE1 knock-in (APE1^{WT}) clones were treated with doxycycline for 9 days to silence endogenous APE1 protein and to express an ectopic FLAG-tagged recombinant shRNA resistant form (APE1^{WT}). Anti-APE1 antibody was used to detect both endogenous and ectopic APE1, while the anti-FLAG was used to confirm the presence of ectopic APE1 in the mitochondrial compartment. LSD1 and ATPVA were used as nuclear and mitochondrial markers, respectively. (B) qRT-PCR analysis of mtDNA content performed on HeLa cell clones. (**: $p < 0.01$). (C) qRT-PCR analysis of mitochondrial polycistronic transcript on HeLa cell clones. (*: $p < 0.05$; **: $p < 0.01$). (D) EMSA performed using increasing concentration of recombinant wild type APE1 protein (rAPE1) and a 29-mer ssRNA with the sequence of mitochondrial COX2 mRNA. (E) Quantification of AP-sites in mt-mRNA of ND1, CytB, COX2, and ATP8/6 after AMA treatment. Precipitated AP-RNA and total RNA were subjected to qRT-PCR, and levels of mt-mRNA damage were determined based on the difference in Ct value between oxidized and total RNA. Data are reported as relative to untreated cells (Ctrl) that were arbitrarily set to 1. (*: $p < 0.05$; **: $p < 0.01$). (F) Representative images of the PLA analysis (*top*) performed to evaluate the interaction between APE1 and RNA under basal condition and upon induction of mitochondrial oxidative stress. PLA was performed using anti-APE1 and anti-BrdU antibodies. Box plot (*bottom*) shows the number of PLA dots counted in an average of 35 cells for each condition of two biological replicates; the differences were significant at a *p*-value of 0.01×10^{-15}. White bars indicate a measure of 10 μm. (G) FLAG-tagged APE1 was immunoprecipitated from recombinant stable clone (APE1^{WT}) treated or not with AMA and eluates were analyzed via qRT-PCR for the presence of mt-mRNAs. Scramble clone was used as mock control and data are reported as relative to untreated cells (APE1^{WT}) that were arbitrarily set to 1. (*: $p < 0.05$; **:$p < 0.01$).

mRNAs are not bound by APE1. Altogether, our analyses confirm that APE1 is able to bind mt-mRNAs and that the binding is increased when mt-mRNAs are damaged as a consequence of mitochondrial oxidative stress.

Mitochondrial APE1 fraction exerts enzymatic activity on mt-mRNA species

The majority of APE1 is localized within the nucleus, where the protein exerts endonuclease activity on abasic DNA but also regulates, in a redox-dependent manner, the activity of several transcriptional factors. Having demonstrated the ability of APE1 to bind mt-mRNA, we decided to verify if mtAPE1 is able to exert endoribonuclease activity on these RNA species, and how this may affect mitochondrial mRNA expression. To confirm that all effects so far described could be ascribed to the mitochondrial APE1 rather than to its nuclear counterpart, we transiently re-expressed on the background of the APE1 shRNA clone an ectopic shRNA-resistant APE1 form where the NLS at N-terminus was replaced by the MTS of MnSOD2.[40,41] In this way, all APE1 present within the cell does localize into the mitochondrial matrix. The Western blot analysis confirmed the expression of the two chimeric proteins: the enzymatically active MTS-APE1^{WT} and the mutant MTS-APE1^{E96A} with a reduced nuclease activity[13] (Figure 2(A)). Through immune fluorescence analysis, we proved that substitution of NLS with MTS led to the exclusion of the recombinant proteins from the nuclear compartment and their accumulation within the mitochondria (Figure 2(B)). Finally, we performed an endoribonuclease assay using recombinant APE1 wild-type (rAPE1^{WT}) and E96A (rAPE1^{E96A}) recombinant proteins (Supplementary Figure S1) and, as a probe, the same RNA sequence of mitochondrial COX2 used in the EMSA analysis (Figure 1(C)), where the only guanosine present within the sequence was substituted by an AP-site. The assay confirmed that APE1 does exert endonuclease activity on an RNA substrate and that the E96A mutant had a significantly lower enzymatic activity (Figure 2(C)).

To assess if the reduction of APE1 nuclease activity could affect mRNA stability, Northern blot analyses were performed using strand-specific riboprobes for ND1 and COX2 mt-mRNAs. In both cases, mRNA levels were higher in APE1-deficient cells and the phenotype was restored at basal levels by sole re-expression of APE1^{WT} within the mitochondrial compartment (MTS-APE1^{WT}). In the endonuclease defective form MTS-APE1^{E96A} the levels of both mRNAs were comparable to that of the shRNA clone (Figure 2 (D)).

In conclusion, data obtained in a cellular system where APE1 was expressed only within the mitochondrial compartment, without the contribution of the nuclear form, indicate that the levels of mt-mRNAs correlate to the expression and endoribonuclease activity of APE1 on mitochondria, suggesting a possible role of APE1 in degradation processes of damaged mt-mRNAs.

Loss of APE1 expression determines increased levels of mt-mRNAs but with higher degree of damage.

To investigate the hypothesis of a direct involvement of APE1 in the metabolism of mt-mRNA, we measured the levels of mitochondrial- (ND1, ND5, CytB, COX2, ATP8/6) and nuclear- (NDUFA1, UQCRC2, CYC1, COX6B, ATPVA) encoded mRNAs codifying for proteins of the complexes I, III, IV, and V, respectively. While the expression of APE1 did not affect the levels of the nuclear-encoded mRNAs, all mitochondrial-encoded transcripts were significantly upregulated in the APE1 shRNA clone. Importantly, re-expression of APE1^{WT} restored the levels of all five mt-mRNAs (Figure 3(A)). To exclude the possibility that the observed effect was due to the use of stable cell clones, HeLa cells were transiently transfected with a different APE1-specific siRNA (Figure 3(B), *top*). Also in this case, APE1 depletion was followed by a significantly increased expression of mitochondrial-encoded mRNAs (Figure 3(B), *top*). Any significant variation was observed for the nuclear-encoded genes (full panel in Supplementary Figure S3). Moreover, to prove that this was a general phenomenon not cell-line dependent, APE1 was transiently silenced in the neuroglioblastoma cell line SF767 (Figure 3(B), *bottom*). In accordance with the previous data, mt-mRNAs levels were significantly increased in APE1 knockdown cells (Figuer 3(B), *bottom*) while nuclear-encoded genes remained unchanged (full panel in Supplementary Figure S3).

Considering that reduced levels of APE1 expression determine a stress condition for the mitochondrion, we evaluated the quality of the same mitochondrial- and nuclear-encoded mRNAs in terms of AP-sites content. Although the levels of all mtDNA-encoded mRNAs analyzed were higher in APE1 shRNA cells (Figure 3(A)), the same mRNAs were more damaged, with a significantly higher number of AP-sites. Also in this case, the phenotype was completely reverted by the re-expression of APE1. No significant variations were observed for the nDNA-encoded mRNAs (Figure 3(C)). To further support the evidence linking the enzymatic activity of mtAPE1 with the amount of mt-mRNAs and the amount of AP-sites, SF767 cells were treated for 3 h and 12 h with APE1′s endonuclease inhibitor Compound #3, which acts as a competitive inhibitor by binding the catalytically active site of APE1.[42] In accordance with the previous results, the levels of all mitochondrial DNA-encoded mRNAs increased as a consequence of APE1

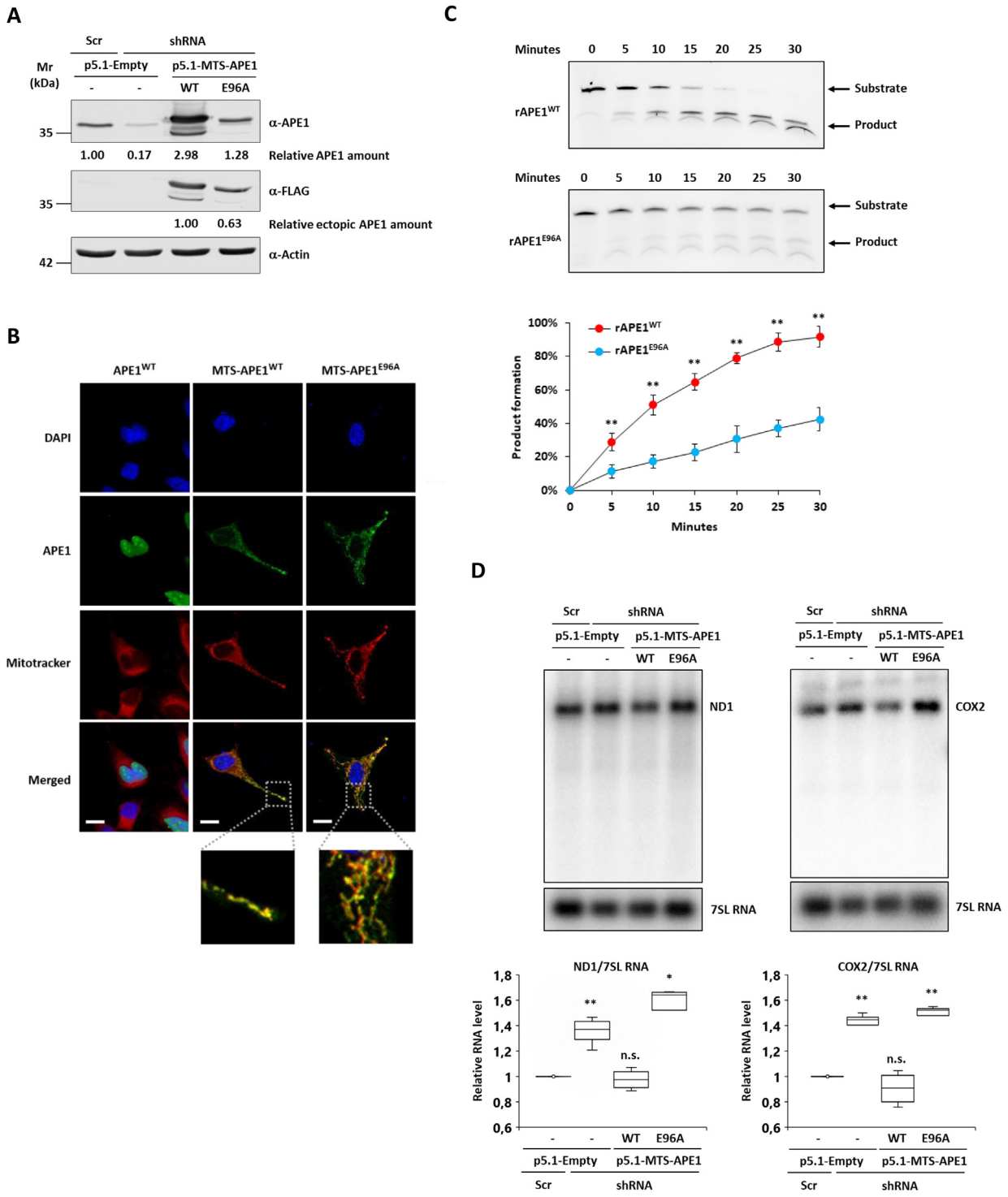

endonuclease inhibition, while nuclear-encoded mRNAs were not affected. The only mRNA for which levels were significantly reduced was ATPVA, but we do not have an explanation for this (Figure 3(D)).

Having proved in different models that loss of mitochondrial APE1 expression or inhibition of its endonuclease activity determines the accumulation of mt-mRNAs with AP-sites, to establish whether the observed rise in mt-mRNA levels was the consequence of an enhanced transcription or of an impairment in the RNA degradation processes, we measured the stability of mt-mRNAs. To do so, ND1, CytB, COX2, and the bicistronic ATP8/6 transcripts of control (Scr), APE1 shRNA, and knock-in ($APE1^{WT}$) clones were measured by metabolic labeling with 4-thiouridine (4sU), as previously described.[43] Loss

of APE1 expression significantly increased the half-lives of examined mt-mRNAs and the effect was rescued by the re-expression of the protein (Figure 3 (E)). Altogether, these data support the hypothesis of a possible role of the mitochondrial form of the APE1 protein in the metabolism of damaged mt-mRNA.

Loss of mitochondrial APE1 negatively affects mitochondrial translation

To thoroughly investigate the effects of APE1 silencing on mitochondrial behavior, we evaluated the downstream effects of the increased mtDNA and mtRNA contents. To assess the consequences of higher levels of mtRNAs but carrying a higher number of AP-sites, we analyzed the mitochondrial translation products. HeLa clones were treated with emetine to selectively block cytoplasmic translation, and then incubated with Met^{35S} for one hour to label newly synthetized mitochondrial polypeptides. Samples were separated on SDS-PAGE and protein expression profile was visualized by autoradiography (Figure 4(A) and (B), *left*). Densitometry analysis was performed to measure the levels of ND1, ATP6, and ND6 proteins, and confirmed significantly impaired expression in APE1 shRNA that was rescued in the $APE1^{WT}$ clone (Figure 4(A), *right*).

Then, we evaluated the protein products of mt-mRNAs by western blot analyses. Experiments were performed on control (Scr), APE1-defective (shRNA), and knock-in ($APE1^{WT}$) clones using specific antibodies for nuclear and mitochondrial DNA-encoded proteins belonging to Complex I (NDUFA1, NDUFS1, ND5), Complex II (SDHB), Complex III (UQCRC2, CytB), Complex IV (COX6B, COX2), and Complex V (ATPVA, ATP6). As a positive control, cells were also treated with chloramphenicol (CHF) for 24 hours to selectively inhibit mitochondrial protein translation.[44] Although after APE1 silencing the levels of mtDNA and mt-mRNAs were higher in shRNA cells (Figures 1(B) and 3(A)), we observed a significant reduction of all investigated mtDNA-encoded proteins (ND5, CytB, COX2, ATP6) (Figure 4(B), *left*). Concerning the nDNA-encoded polypeptides belonging to the respiratory complexes, with the exception of Complex V, their expression was affected by APE1 levels as well. This result could be explained considering that the assembly of the oxidative phosphorylation (OXPHOS) system is an intricate process that requires the insertion of mtDNA-encoded subunits into the inner membrane of mitochondria, in concert with tens of subunits encoded by nuclear genes.[45] Reduced expression of mtDNA-encoded genes could alter the stability of all OXPHOS subunits, as in the case of complexes III and IV that serve as an anchor at the membrane to recruit Complex I into the respiratory chain.[46,47] Indeed, the positive control treatment with CHF also elicited a reduction of mitochondrial- and nuclear-encoded proteins (Figure 4(B), *right*). This surprising result led us to hypothesize that dysfunction of APE1 increases the levels of damaged mt-mRNAs, which are no longer available for the protein synthesis.

APE1 controls OXPHOS complex stability and mitochondrial respiration

Considering that all 13 mitochondrial-encoded polypeptides are components of the respiratory complexes I, III, IV and V, we evaluated the effect of APE1 loss of expression on mitochondrial respiration by examining the formation and stability of OXPHOS complexes and the respiratory parameters. BN-PAGE analyses

Figure 2. Mitochondrial APE1 exerts endoribonuclease activity on mRNA. (A) Western blot analysis of control (Scr) and APE1 shRNA clones treated with doxycycline and transiently transfected with empty vector (p5.1-Empty) or FLAG-tagged expression plasmids codifying for shRNA-resistant APE1 forms MTS-$APE1^{WT}$ and MTS-$APE1^{E96A}$. Anti-APE1 and anti-FLAG antibodies were used to detect endogenous and ectopic APE1 expression, respectively. Anti-Actin was used as a loading control. (B) Representative images of immunofluorescence analysis of APE1 shRNA clone transiently transfected with FLAG-tagged expression plasmids codifying for shRNA-resistant $APE1^{WT}$ and mitochondrial targeted mutants MTS-$APE1^{WT}$ and MTS-$APE1^{E96A}$. Nuclei were stained with DAPI, APE1 with anti-FLAG conjugated with 488 dye, and mitochondria with MitoTracker Deep Red. White bars indicate a measure of 10 μm. A 10-μm-square area has been highlighted on merged images of MTS cells and electronically enlarged 3.5 times to show the co-localization between APE1 and MitoTracker. (C) Representative gel images of endonuclease activity on AP-RNA of $APE1^{WT}$ and $APE1^{E96A}$ mutant (*top*) and diagram showing the difference in the kinetics of the two proteins (*bottom*). 2.5 pmol of AP-RNA were incubated with 150 ng of recombinant APE1 proteins for the reported amount of time. (**: $p < 0.01$). (D) Northern blot analysis of RNA isolated from control (Scr) and APE1 shRNA clones treated with doxycycline and transiently transfected with empty vector (p5.1-Empty) or FLAG-tagged expression plasmids codifying for MTS-$APE1^{WT}$ and MTS-$APE1^{E96A}$. Mitochondrial-encoded ND1 (*left*) and COX2 (*right*) mRNAs were detected with the help of strand-specific radiolabeled riboprobes. Nuclear-encoded 7SL RNA was used as a loading control. Representative autoradiograms are shown (*top*). Box plots (*bottom*) show quantitation and mean ± SD of four biological replicates. Statistical significance was calculated with respect to the control sample (Scr-Empty). (n.s.: not significant; *: $p < 0.05$; **: $p < 0.01$).

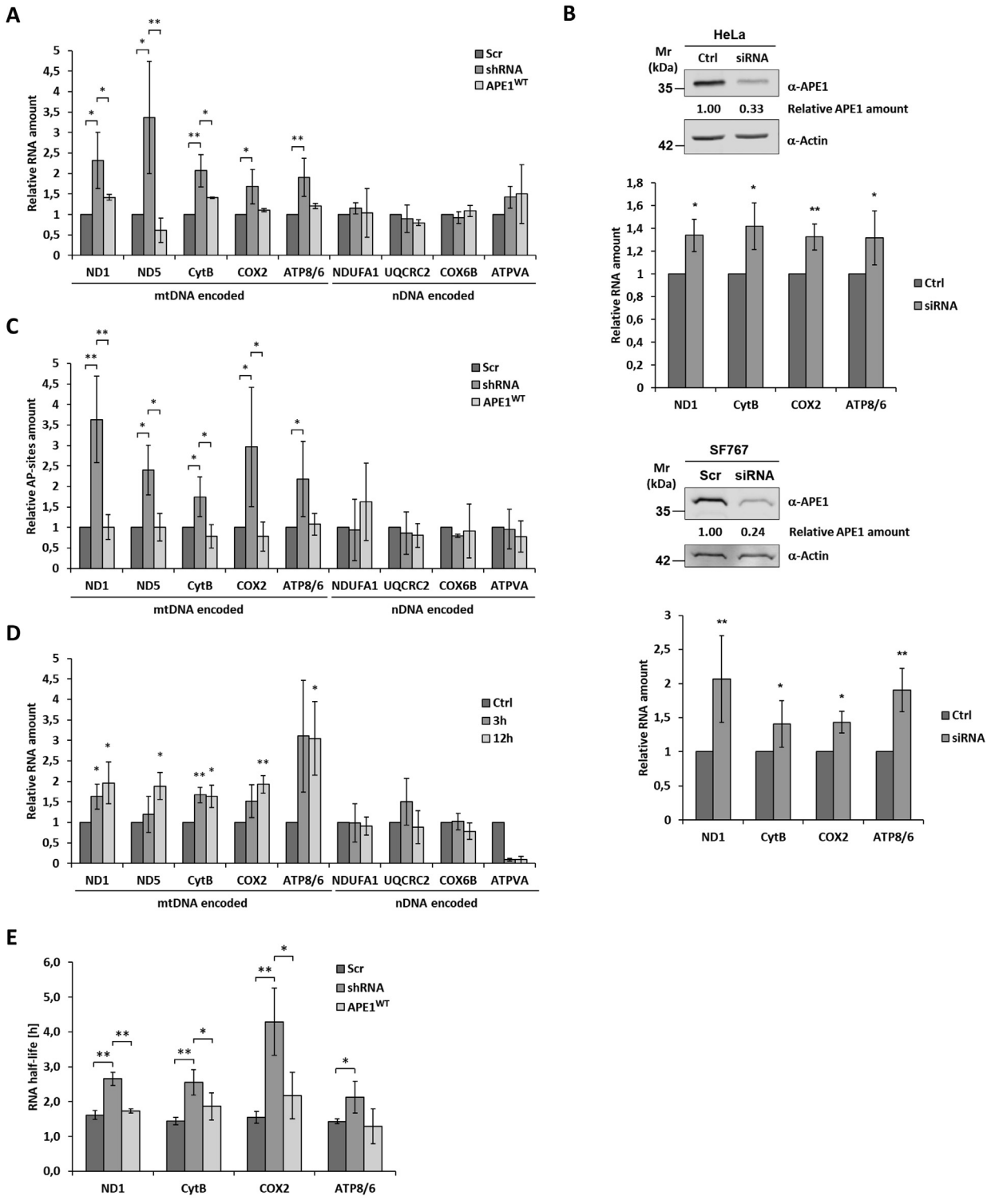

highlighted the reduction in the stability of respiratory complexes I and III, while we did not observe any significant difference in Complex V (Figure 5(A)). Complex I is composed of seven mitochondrial-encoded subunits (ND1, ND2, ND3, ND4, ND4L, ND5, ND6) that constitute its transmembrane domain. This explains how even modest reductions in the expression levels of its subunits can affect its assembly and stability. Complex III is a small complex composed of ten nuclear and only one mitochondrial-encoded protein (CytB) but which is in the core of the complex and represents the complex's central catalytic subunit. Therefore, it is not surprising that

the biogenesis of this complex is impaired when the level of CytB is reduced. On the other hand, Complex V is a large complex composed of 29 proteins, two of which (ATP6 and ATP8) are mitochondrial encoded. However, it has been demonstrated that although the ATP6 mutation inhibits and destabilizes Complex V, it does not prevent the assembly and oligomerization of the complex.[48] In line with that, we did not observe the affected assembly of Complex V.

To provide the last proof for the important role of APE1 in mt-mRNA metabolism and its contribution to the respiratory function of mitochondria, we conducted Seahorse analyses to measure the respiratory parameters. Data confirmed significantly reduced basal respiration (60 ± 10%), maximum respiration (62 ± 22%), and ATP production (53 ± 4%) in the APE1 shRNA clone as well as demonstrated that all parameters were efficiently rescued by the re-expression of $APE1^{WT}$ (Figure 5(C)). Moreover, correlating the oxygen consumption rate with the media acidification rate of the clones, we also obtained the energy state description of the cells.[49,50] After APE1 silencing there is a significant shift of the energetic state towards the glycolytic phenotype (less ATP production and more proton release), while $APE1^{WT}$ completely reverts the phenotype, bringing the cells again to a more energetic state (Figure 5(D)).

Discussion

Since its discovery in the early 90 s, APE1 has been widely studied for its essential role as a DNA repair protein and as a redox activator of transcriptional factors controlling cell growth and apoptotic pathways. Over the years, research on APE1 has been mainly associated with its role in tumorigenic processes and tumor resistance, making it a target for combinatory anticancer therapies.[51] More recent is the discovery of this protein's presence within the mitochondrial matrix[21,33] and its participation in the BER pathway.[52] Nevertheless, for many years the scientific community's interest in this pleiotropic protein has been mainly focused on the nuclear form, with less attention paid to endonuclease activity of APE1 in the mitochondrial DNA. In the last decade, however, more research groups have directed their studies toward the biological relevance of APE1 extra-nuclear localization in association with the phenomena of tumor resistance in lung carcinoma,[53] hepatocellular carcinoma,[41,54] rectal cancer,[55] and more, as well as the characterization of uncanonical functions of this DNA repair enzyme, such as its endoribonuclease activity.[14,15,18,56]

Loss of APE1 expression determines cellular stress and in particular, mitochondria seem to be very sensitive to the absence of this protein. It was demonstrated in different diseases and cellular models that APE1 silencing leads to increased mtDNA damage, drop of mitochondrial potential, increased cytochrome *c* release in the cytoplasm, higher caspase 3/7 activity, and excessive production of ROS.[34,35,57–59] Moreover, when cells are challenged with oxidative or alkylating agents (e.g.: H_2O_2, rotenone), silencing of APE1 emphasizes these effects, impairing the response to oxidative stress and inducing apoptosis.[57,58] Interestingly all these effects were for the major part ascribed to the mitochondrial fraction of APE1. In fact, we already showed that cells expressing the C65S mutant form of the protein, whose mitochondrial import is impaired, are not able to rescue the membrane potential drop of mitochondria after endogenous APE1 silencing.[33] Joo and colleagues also demonstrated that in endothelial cells APE1 knockdown increased the sensitivity to PKC-induced mitochondrial dysfunction, increasing the mitochondrial hyperpolarization and

Figure 3. Mitochondrial mRNA half-life is dependent on APE1 expression levels. (A) qRT-PCR analysis of mitochondrial DNA (ND1, ND5, CytB, COX2, ATP8/6) and nuclear DNA (NDUFA1, UQCRC2, COX6B, ATPVA) encoded mRNAs on control (Scr), APE1 shRNA, and APE1 knock-in ($APE1^{WT}$) clones. Results shown in the graph are the mean ± SD of four biological replicates. Statistical significance was calculated with respect to the control sample (Scr). (*: $p < 0.05$; **: $p < 0.01$). (B) Representative Western blot analysis of total cellular extract of HeLa cells (*top*) and SF767 cells (*bottom*) transiently transfected with control (Scr) and specific siRNA for APE1. Protein expression was evaluated using anti-APE1 antibody, while anti-Actin was used as a loading control. qRT-PCR analysis of mitochondrial DNA encoded mRNAs expression of HeLa (*top*) and SF767 (*bottom*) cells where APE1 protein was transiently silenced by siRNA transfection. (*: $p < 0.05$; **: $p < 0.01$). (C) Quantification of AP-sites in mitochondrial- and nuclear-DNA encoded mRNAs on control (Scr), APE1 shRNA, and APE1 knock-in ($APE1^{WT}$). Precipitated AP-RNA and total RNA were subjected to qRT-PCR, and levels of mt-mRNA damage were determined based on the difference in Ct value between oxidized and total RNA. Data are reported as relative to scramble clone that was arbitrarily set to 1. Data reported are the mean ± SD of four independent biological replicates. (*: $p < 0.05$; **: $p < 0.01$). (D) qRT-PCR analysis of mitochondrial- and nuclear-DNA encoded mRNAs in SF767 cells treated for 3 and 12 hours with APE1's endonuclease inhibitor Compound #3. (*: $p < 0.05$; **: $p < 0.01$). (E) Graph showing the mitochondrial-encoded ND1, CytB, COX2, and ATP8/6 mRNAs half-life calculated by metabolic labeling with 4-thiouridine (4sU). Data reported are the mean ± SD of four independent biological replicates. (*: $p < 0.05$; **: $p < 0.01$).

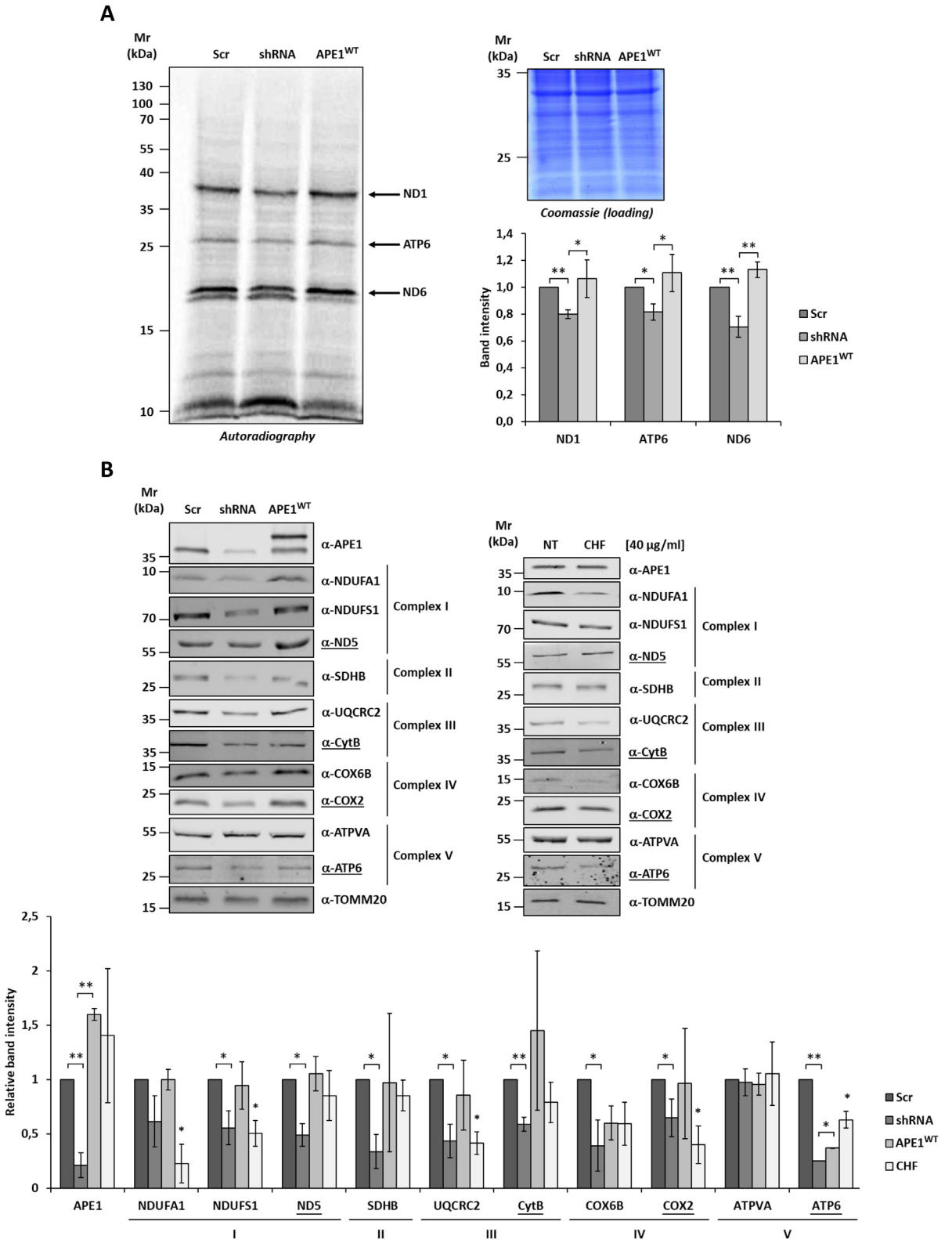

mitochondrial ROS production. This phenotype was rescued by the expression of an ectopic form of APE1 carrying an MTS sequence and driving the protein directly to the mitochondrial matrix.[58] Interestingly, expression of MTS-APE1 was able to better counteract the detrimental effects of endogenous APE1 silencing than the wild-type form of the protein.

Our research offers a completely new point of view in the study of APE1 and provides, for the first time, direct proof of the essential role of this protein in mitochondrial RNA biology. The present work unveils that, in mitochondria, APE1 is associated to mRNAs and that oxidative stress conditions enhance this binding. The oxidative modification of bases has been reported to be a major oxidative modification of DNA.[60] AP-sites represent the substrates of APE1 and can be chemically generated by damaging or oxidizing agents such as alkylating agents or ionizing radiation. In addition, AP-sites are intermediates in the repair pathway initiated to eliminate oxidized bases by DNA glycosylases.[61] As for the DNA, RNA can also undergo oxidative damage, forming 8-OHG. Unfortunately, there have been few studies regarding biochemical analysis of base oxidation, and overall, the general source of AP-sites in RNA is poorly understood. The 8-oxoguanosine glycosylase has been found within the mitochondrial matrix and it is capable of base excision in DNA, but so far it has never been proved to be active on ssRNA. Very recently, for the DNA glycosilases, SMUG1′s ability in recognizing and removing modified RNA substrates has been demonstrated.[62] Unfortunately, this enzyme has never been proved to be present within the mitochondrial matrix.[63] Therefore, a possible explanation for the formation of AP-sites in mitochondrial RNA could be ascribed to direct depurination as proposed by Tanaka and colleagues.[36] Further studies are needed to shed light on these biological processes.

In our work the measurements of mt-mRNA AP-sites confirmed significantly higher levels of AP-RNA in the absence of APE1 and a direct correlation between the levels of APE1 in mitochondria and the half-life of mt-mRNAs. These data suggest a leading role of the mitochondrial form of APE1 in the degradation processes of damaged mt-mRNA. To support this hypothesis, rescue experiments were performed on the background of APE1 knockout cells by re-expressing a recombinant form of the protein that was targeted only into the mitochondrial matrix. Data confirmed that mRNA's half-life was significantly longer in the absence of mitochondrial APE1 as a result of impaired degradation processes due to the loss of APE1 expression or re-expression of the endonuclease-defective mutant E96A.

Next, we correlated the expression levels of APE1 with the downstream effects, showing that impaired removal of damaged mt-mRNAs affects assembly/stability and functioning of the respiratory complexes.

Information about the mitochondrial RNA degradation process is still scanty. The most well-characterized complex able to degrade the mt-mRNAs in the mitochondrial compartment is the PNPase/SUV3 complex, also called the degradosome.[31] PNPase is a polynucleotide phosphorylase capable of 3′-to-5′ phosphorolysis and 5′-to-3′ RNA polymerization,[64] while SUV3 is an NTP-dependent RNA and DNA helicase; both proteins were shown to localise in the mitochondrial RNA granules (MRGs).[65,66] It has been proposed that this complex exerts its function in a specific subcompartment of MRGs called D-foci, where diverse RNAs species and the degradosome localize.[31] In particular, Szczesny *et al.* showed that SUV3 is required for the degradation of the antisense mtRNAs and is involved in the decay of sense mitochondrial transcripts.[30] PNPase cooperates with SUV3 in mtRNA surveillance; however, this enzyme seems to have a wider role in mitochondria because PNPase has dual matrix-intermembrane space localization.[67]

On the basis of our data, we are proposing a molecular model for the degradation of damaged mitochondrial mRNA. Presence of AP-sites derived by the exposure to ROS determines the stall of the mitoribosome and consequently of the mitochondrial translation. APE1 acts by binding and degrading damaged mRNA restoring translation processes and, as a downstream effect, maintaining OXPHOS capacity. In contrast, in the absence of APE1, AP-sites accumulate, determining the block of mitochondrial translation and determining a significant loss of respiratory capacity (Figure 6). To the best of our knowledge, this represents the first evidence of a mechanism involved in the degradation of damaged mRNA in mitochondria. We do not exclude, in association

Figure 4. APE1 levels affect mitochondrial translation. (A) Representative autoradiography image (*left*) and Coomassie staining (*right, top*) of SDS-PAGE electrophoresis of mitochondria translation analysis of control (Scr), APE1 shRNA and knock-in ($APE1^{WT}$) clones after emetine/^{35}S treatment. Bands corresponding to ND1, ATP6, and ND6 were quantified and data were reported in the graph as relative to control clone. Coomassie staining was used as loading control. (*: $p < 0.05$; **: $p < 0.01$). (B) Western blot analysis (*top, left*) of total cell extract of control (Scr), APE1 shRNA and knock-in ($APE1^{WT}$) clones treated with doxycycline for 9 days. Specific antibodies for Complex I (NDUFA1, NDUFS1, ND5), Complex II (SDHB), Complex III (UQCRC2, CytB), Complex IV (COX6B, COX2) and Complex V (ATPVA, ATP6) proteins were used. Anti-TOMM20 was used as a loading control. As a positive control, cells were treated with chloramphenicol (CHF) for 24 hours to inhibit mitochondrial translation (*top, right*). Graph (*bottom*) reports densitometric analyses of each protein relative to the control sample. mtDNA encoded proteins are underlined. Data reported are the mean ± SD of four independent biological replicates. (*: $p < 0.05$; **: $p < 0.01$).

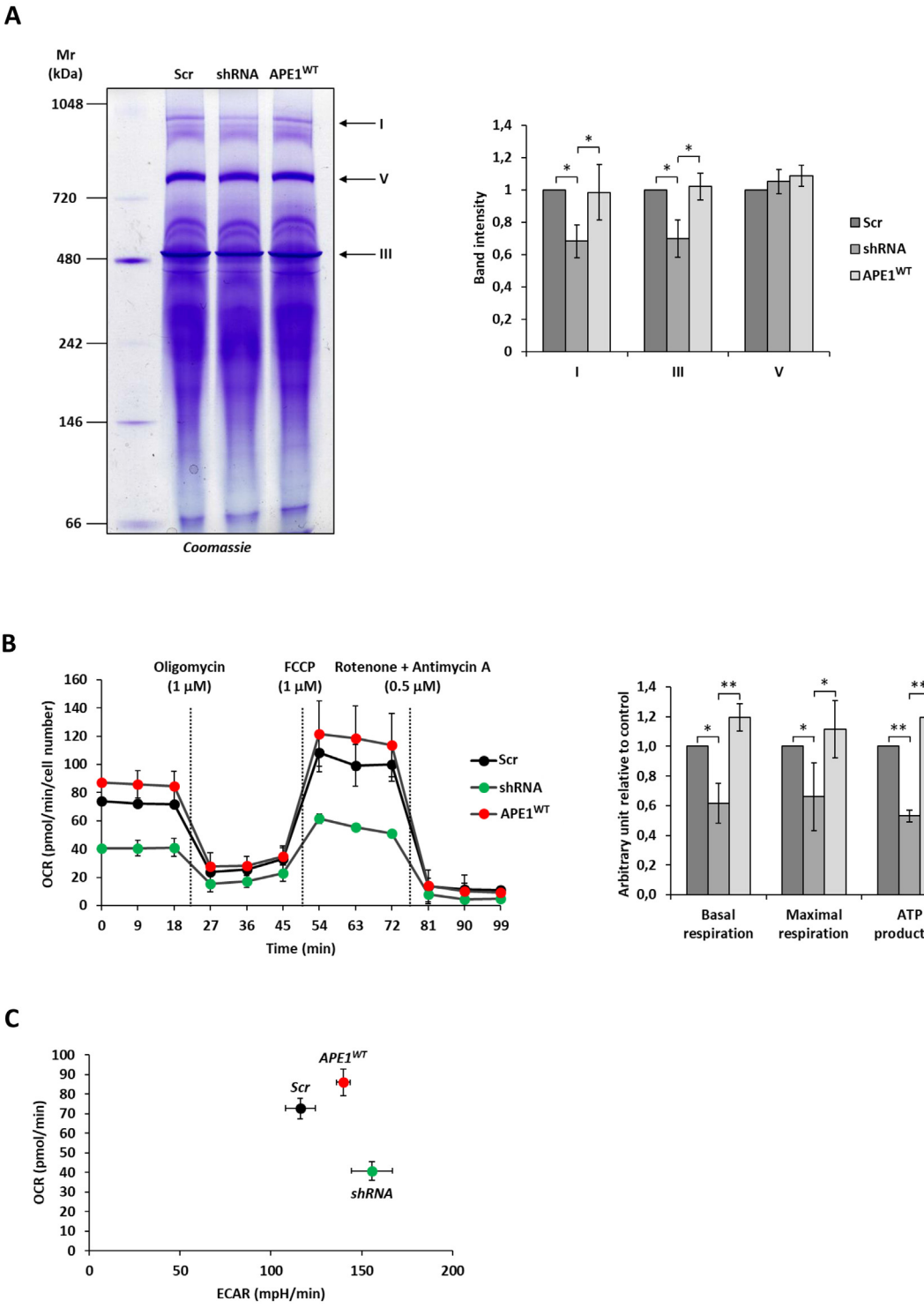

with APE1, the involvement of other factors in this complex biological process that will require further specific investigations. Currently, there is no evidence in the literature that APE1-mediated processing of AP-sites within mRNA transcripts occurs co-translationally. However, a preliminary interactome analysis of mitochondrial APE1 performed in our laboratory revealed the presence of several mitochondrial proteins belonging to the large and small mitochondrial ribosomal subunits (e.g. MRPL9 and MRPS15), suggesting that the degradation process may occur co-translationally or in close proximity to the mitochondrial ribosomes. Again, further specific studies are required to elucidate the molecular details of this biological process.

An alternative explanation for the increased RNA levels observed when APE1 is downregulated is the upregulation of transcription rather than a downregulation of APE1-mediated RNA transcript processing. However, conclusions driven by our experiments strongly suggest a role for APE1 in the degradation process of damaged mt-mRNA. The E96A mutant has reduced enzymatic activity and therefore cannot efficiently process/degrade damaged mRNA. If downregulation of APE1 determined an increased transcription, we would not have observed this effect when this mutant form was expressed. Consistent with these data, we should not have observed increased levels of mt-mRNA species even when using the endonuclease inhibitor Compound #3 (Figure 3 (D)). In addition to this evidence, what further supports our hypothesis of APE1-mediated RNA transcript processing is that we measured higher levels of AP-site on mt-mRNAs in the absence of APE1 (Figure 3(C)) and that the half-life was significantly longer (Figure 3(E)).

In summary, this study not only confirms and extends the emerging role of APE1 in RNA biology, but also reveals, for the first time, a new function of the mitochondrial form of this protein in mitochondrial metabolism. Therefore, in the light of this observation, all data regarding the extra-nuclear localization of APE1 in correlation with tumorigenesis and tumor resistance could be re-interpreted considering APE1 as not only a DNA repair protein but also as a key component of the mitochondrial RNA degradosome.

Materials and Methods

Further details about preparation of cell extracts, recombinant proteins expression and purification, EMSA and endonuclease assay, and mtDNA quantification are provided in the Supplementary Data.

Cell culture and treatments

For inducible silencing of endogenous APE1, HeLa cell clones were developed as described in Vascotto *et al.*[33] To induce APE1 silencing, doxycycline (Sigma Aldrich) was added to the cell culture medium at the final concentration of 1 μg/mL, and cells were grown for 9 days. For RNA labeling, cells were grown in complete DMEM with BrU 2.5 mM for 30 min with or without the presence of AMA 25 μM. Then, the cells were fixed with 4% (W/V) paraformaldehyde and used for immunofluorescence analysis. Inhibition of endonuclease activity of APE1 was achieved by treating cells with Compound #3.[42] SF767 cells were treated with 10□M of Compound #3 for 3 or 12 h in DMEM supplemented with 10% FBS, 1% Glutamine and 1% penicillin/streptomycin.

Transient transfection experiments

For APE1 transient silencing, one day before transfection, HeLa cells were seeded in 10 cm plates at the density of 1.2×10^6 cells/plate. They were then transfected with 100 nM of control (Scr) [5′-CCAUGAGGUCAGCAUGGUCUG-3′ for the top strand and 5′-AAGGUACUCCAGUCGUAC CAG-3′ for the bottom strand] and APE1 (siRNA) [5′-GUCUGGUAAGACUGGAGUACC-3′ for the top strand and 5′-UACUCCAGUCUUACCA GACCU-3′ for the bottom strand] siRNA per plate using Oligofectamine 2000 (Invitrogen) according to the manufacturer's instructions. Cells were harvested 72 h after the transfection for proteins and mRNA analyses. To target APE1 only in the mitochondria compartment, the N-terminal 20 amino acid residues of APE1 carrying the NLS (nuclear localization signal) were replaced with the MTS (mitochondrial targeting sequence) of the human mitochondria-specific Mn^{2+}-superoxide dismutase (MnSOD) gene as previously described.[40,41] Then, MTS-APE1^{WT} and MTS-APE1^{E96A} cDNAs were cloned into the pCMV5.1-FLAG expressing vector. Scr and shRNA cells were treated with doxycycline for 7 days, then 4.5×10^6 cells/plate were seeded 24 h before transfection. Cells were then transfected with 12 μg of pCMV5.1-MTS-APE1^{WT}, pCMV5.1-MTS-APE1^{E96A} or empty vector per plate using Lipofectamine 2000 (Invitrogen) according to the manufacturer's instructions. Cells were harvested 24 h after the transfection.

Figure 5. APE1 levels affect mitochondrial respiration. (A) Coomassie staining of mitochondrial respiratory complexes from Scr, shRNA and APE1^{WT} clones after BN-PAGE electrophoresis (*left*). Bands corresponding to complexes I, III, and V are quantified and data relative to the control sample are reported in the graph (*right*). (*: $p < 0.05$). (B) Oxygen consumption rate evaluation of control Scr, shRNA and APE1^{WT} clones. Basal OCR was first evaluated, then cells were treated with the reported amounts of oligomycin, FCCP, rotenone and antimycin A, and OCR was measured three times after each injection. Diagram reports the OCRs of the clones relative to the Scr clone (*top*). Graph (*bottom*) reports the basal respiration, maximal respiration, and ATP production capacity of clones extrapolated from the diagram. (*: $p < 0.05$; **: $p < 0.01$). (C) Oxygen consumption rates/extracellular acidification rates ratios were evaluated for Scr, shRNA and APE1^{WT} clones. OCR/ECAR ratios were calculated considering mean values of the basal respiration, two-variables graph reporting OCR in Y axis and ECAR in X axis, for the evaluation of the energetic state of the clones after APE1 silencing and APE1^{WT} re-expression.

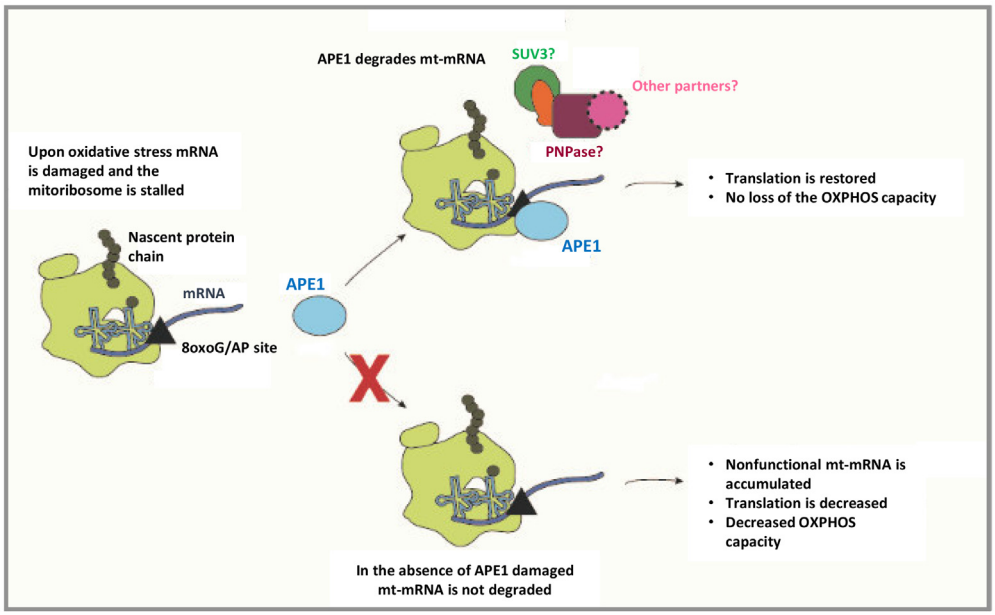

Figure 6. Proposed model depicting the contribute of APE1 in the degradation process of damaged mt-mRNA. Upon oxidative stress, mt-mRNAs are damaged, leading to stalling of the mitochondrial ribosome. APE1 binds and cleaves the abasic RNA, restoring the translation. In contrast, in the absence of APE1 nonfunctional damaged mRNAs accumulate and mitochondrial translation is impaired, determining a decrease of the respiratory efficiency.

Western blot analysis

The indicated amounts of total cell extract (TCE) or mitochondrial extract (MCE) were separated onto 12% SDS-PAGE. Then, proteins were transferred to nitrocellulose membranes (Schleicher & Schuell). Membranes were saturated by incubation with 5% nonfat dry milk in PBS/0.1% Tween 20 at room temperature for 1 h and incubated with the specific primary antibody. Primary antibodies are listed in the Supplementary Data, Table S1. Membranes were washed three times with PBS/0.1% Tween 20 and incubated with the secondary antibody (IRDye 680 and IRDye 800) (LI-COR Biosciences) 1:10000 for 2 h. After three washes with PBS/0.1% Tween 20, signals were detected with an Odyssey CLx scanner (Li-Cor Biosciences). LSD1 and ATPVA were used as nuclear and mitochondria markers, respectively. Normalization of mitochondria protein extract (MCE) was performed with anti-TOMM20. Blots were then quantified using ImageStudio software (Li-Cor Biosciences).

Mitochondria isolation

10×10^7 cells were seeded one day before the procedure. After 24 h, cells were washed twice with PBS and detached by scraping. After an additional wash, the cells were centrifuged at 250*g* and 4 °C for 5 min. Next, they were resuspended in 12 mL of MIB buffer [20 mM HEPES pH 7.6, 1 mM EDTA pH 7.4, 220 mM mannitol, 70 mM sucrose, 2 mg/mL BSA, 0.5 mM PMSF] and gently homogenized into a glass-glass potter with 20 strokes. Then, the suspension was transferred into a falcon tube and centrifuged at 650*g* and 4 °C for 5 min. The supernatant containing mitochondria was removed and kept on ice while the pellet, containing nuclei and unbroken cells, was homogenized again with 10 strokes to increase the final yield. The suspension was centrifuged again at 650*g* and 4 °C for 5 min. The two supernatants were pooled together and centrifuged once again at 650*g* and 4 °C for 5 min. The supernatant was carefully removed and centrifuged at 14,000*g* and 4 °C for 15 min while the pellet, containing mitochondria, was washed with MIB buffer supplemented with 1 M KCl to remove proteins and nucleic acids attached to the outer membranes of mitochondria and then centrifuged at 14,000*g* and 4 °C for 15 min. Finally, mitochondria were washed with MIB buffer w/o KCl and BSA and centrifuged again as before, the supernatant was removed, and the pellet was resuspended in MIB buffer w/o KCl and BSA, keeping mitochondria as concentrated as possible. Sample concentration was determined by using the Bradford reagent.

RNA extraction and qRT-PCR

Total RNA extraction from cells was performed using the NucleoSpin RNA kit (Macherey-Nagel GmbH & Co). 1 μg of total RNA was reverse transcribed using the iScript cDNA synthesis kit (Bio-Rad) according to the manufacturer's instructions. The Minimum Information for

Publication of Quantitative Real-Time PCR Experiments (MIQE) guidelines[68] were used as the basis for establishment of the workflow. qRT-PCR was performed with the iQ5 multicolor real-time PCR detection system (Bio-Rad) according to the manufacturer's protocol and primers listed in the Supplementary Data, Table S2. cDNA was amplified in 96-well plates using the 2X iQ SYBR green supermix (Bio-Rad) [100 mM KCl, 40 mM Tris-HCl pH 8.4, 0.4 mM each deoxynucleoside triphosphate [dNTP], 50 U/mL iTaq DNA polymerase, 6 mM $MgCl_2$, SYBR green I, 20 nM fluorescein, and stabilizers] and 300 nM of the specific sense and antisense primers in a final volume of 15 μL for each well. Each sample analysis was performed in triplicate. A sample without the template served as a negative control. The cycling parameters were denaturation at 95 °C for 10 seconds and annealing/extension at 60 °C for 30 seconds (repeated 40 times). To verify the specificity of the amplification, a melting-curve analysis was performed immediately after the amplification protocol, and PCR products were separated onto 2% agarose gel.

RNA AP-sites quantification

AP-sites were quantified as previously described,[69] with some modifications. Briefly, 10 μg of total RNA were incubated with 2 mM ARP (N-(Aminooxyacetyl)-N'-biotinylhydrazine) in 50 mM Na acetate buffer pH 5.2 for 40 min at 37 °C. As a loading control we used an *in vitro* synthesized RNA encoding Xenopus elongation factor 1α gene, biotinylated at the 5′-end (5′-BIOT-UAG CUCUUGACUGCAUUUUG CCACCAUCU CGCCCAACCGAUAAGCCUCUCCGUCUGCCUC UGCAGGAUGUCUACAAAAUU-3′), that was added to the total RNA after derivatization. Then, RNA was precipitated by ethanol. After resuspension with 10 μL of deionized water, an aliquot of 2 μL was put aside for quantifying total transcripts, and the remaining RNA was incubated with streptavidin magnetic beads for 20 min at 60 °C. Beads were washed twice with solution A [1 M NaCl, 20 mM Tris-HCl pH 7.5, 5 mM EDTA, 1% NP-40], three times with solution B [2 mM Tris-HCl pH 7.5, 0.5 mM EDTA, 1% NP-40], three times with solution C [4 M urea, 10 mM Tris-HCl pH 7.5, 1 mM EDTA, 1% NP-40], and 2 times with solution D [2 mM Tris-HCl pH 7.5, 1 mM EDTA]. Affinity purifyed RNA was dissociated from beads by incubation with 2.5 mM biotin solution at 90 °C for 5 min, precipitated by ethanol, and resuspended in deionized water. Precipitated and total RNA were used for cDNA synthesis (SuperScript™ III Reverse Transcriptase, Invitrogen). Complementary DNA was used for qRT-PCR (SYBR Green Master Mix from Bio-Rad) according to the manufacturer's protocol. Specific primers were designed to amplify mitochondrial (ND1, ND5, COX2, CytB, and ATP8/6) and nuclear (NDUFA1, UQCRC2, COX6B, ATPVA) mRNAs as reported in the Supplementary Data, Table S2. Xen_for and Xen_rev primers were used to amplify the *in vitro* synthesized RNA-encoding Xenopus elongation factor 1α gene. The levels of mRNAs AP-sites were normalized with the amplification of Xenopus elongation factor 1α gene, and levels of damaged mRNA were determined based on ΔCq values between Cq of total RNA (INPUT) and oxidized RNA (IP). Finally, each oxidized RNA sample was expressed as relative amount compared to the scramble (Scr) levels of the same RNA.

Immunofluorescence and PLA

For IF and PLA analyses, cells were seated into a glass coverslip in the amount of 8×10^4 per 24x multiwell plate. The day after, cells were fixed with 4% (w/v) paraformaldehyde for 20 min, permeabilized with Triton X-100 0.5% in PBS 1X for 5 min and incubated with 5% goat serum in Duolink *in situ* Solution A [Blocking solution] (Sigma Aldrich) for 1 h to block unspecific binding of the antibodies. Then, cells were incubated with primary antibody diluted in the Blocking solution in a humid chamber [anti-FLAG monoclonal (Sigma Aldrich) (F1804): 2 h at RT, dilution 1:100; anti-APE1 monoclonal (Novus Biological) (13B8E5C2): 2 h at RT, dilution 1:400; anti-BrdU polyclonal (Thermo Fisher Scientific) (PA5-32256): o/n at 4 °C, dilution 1:400].

For IF analysis, after washing three times with Solution A for 5 min, cells were incubated with secondary antibody conjugated with Alexa Fluor fluorophore (Thermo Fisher Scientific), diluted 1:1000 in Blocking solution for 90 min at RT. Mitochondria were stained before fixation with MitoTracker Deep Red at a concentration of 100 nM for 15 min, followed by three washes in PBS before fixation. Manufacturer's instructions were followed for PLA analyses. Images were acquired using confocal microscope Zeiss Axio Imager Z2 LSM 700. PLA blobs count was performed using the BlobFinder software.

APE1 IP and evaluation of RNA binding

2×10^7 cells were collected and resuspended in 2.5 mL of PBS. The same volume of a solution of 1% formaldehyde in PBS was added to the cells and incubated for 10 minutes at RT while shaking. Formaldehyde cross-linking action was then blocked with glycine 270 mM. Cells were washed twice in PBS and incubated in lysis buffer [Tris-HCl 50 mM pH 7.5; NaCl 150 mM; EDTA 1 mM pH 8.0; Triton X-100 1%; protease inhibitor cocktail] supplemented with 200 U of RiboLock RNAse Inhibitor (Thermo Scientific) for 30 minutes at 4 °C. The lysed samples were centrifuged at 20,000*g* for 20 minutes at 4 °C. 50 μL were collected as INPUT. Lysates were incubated with Anti-FLAG M2 magnetic beads (Sigma-Aldrich) for

3 hours, rocking at 4 °C. Five washes in TBS 1X + RiboLock were followed by elution with peptide FLAG for 30 minutes on orbital shaker, at 4 °C. Supernatants were collected and incubated at 65 °C for 1 hour to reverse the cross-link. Samples were then digested with DNA-free DNA Removal Kit (Invitrogen): 1 μL of DNAse and 5 μL of reaction buffer were added to each sample and the reaction was incubated at 37 °C for 30 minutes. Five μL of DNAse Inactivation Reagent were used to stop the reaction. Samples were centrifuged at 10,000*g* for 2 minutes and supernatants were collected in new tubes. As a loading control we used the *in vitro* synthesized RNA-encoding Xenopus elongation factor 1α gene. To extract RNA, 50 μl of TRIzol™ were added to each sample, mixed, and the reaction was incubated for 2 minutes at RT. After the addition of 50 μl of chloroform, samples were centrifuged at 12,000*g* for 15 minutes, at 4 °C. The aqueous phases, containing RNA, were collected in new tubes. Ten μg of glycogen and 125 μl of isopropanol were included per sample and, after a 12,000*g* centrifugation for 10 minutes at 4 °C, a wash in EtOH 75% was performed. Samples were centrifuged at 7500*g* for 5 minutes at 4 °C and finally pellets were resuspended in 10 μl of RNAse-free water. RNA was resuspended in 10 μl of RNAse-free water and retrotranscribed using the iScript cDNA synthesis kit. Input was diluted 1:20, while the IP sample was diluted 1:10. Finally, a RealTime PCR was performed to amplify mitochondrial ND1, ND5, COX2, CytB, and ATP8/6 and nuclear (NDUFA1, UQCRC2, COX6B, ATPVA) genes. To normalize each sample, Xen_for and Xen_rev primers were used to amplify the *in vitro* synthesized RNA-encoding Xenopus elongation factor 1α gene.

Northern blot analysis

Northern blot analyses were performed essentially as reported by Szczesny and colleagues.[30] 1 μg of RNA was dissolved in denaturing solution [5.5% formaldehyde, 50% formamide, NBC buffer: 50 mM boric acid, 1 mM sodium acetate, 5 mM NaOH], incubated for 5 min at 60 °C and mixed with loading dye [15% Ficoll, 0.1 M EDTA, pH 8.0, 0.25% bromophenol blue, 0.25% xylene cyanol]. The samples were run on a 1% agarose gel containing formaldehyde (0.9%) followed by overnight capillary transfer to Nytran-N membrane (GE Healthcare) in 10 × SSC [1.5 M sodium chloride, 150 mM sodium citrate]. After the transfer, the membrane was washed briefly in 2 × SSC, UV cross-linked, and stained with methylene blue solution [0.02% methylene blue in 0.3 M sodium acetate, pH 5.5]. PCR products containing SP6 promoter sequence corresponding to the mtDNA fragments 3652–4029 (ND1) and 7586–7900 (COX2) were used as templates for preparing strand-specific [α-32P] UTP-labeled (Hartmann Analytic) riboprobes by *in vitro* transcription. For detection of nuclear-encoded 7SL RNA transcript, PCR product of primers 5′-TCGGGTGTCC GCACTAAGTT-3′ and 5′-TGGCTATTCA CAGGCGCGAT-3′ was used as a template for labeling with [α-32P] dATP (Hartmann Analytic) using a DecaLabel DNA Labeling Kit (Thermo Scientific). Hybridizations were performed overnight in PerfectHyb Plus buffer (Sigma) at 65 °C followed by washing. Membranes were exposed to PhosphorImager screens (FujiFilm), and the screens were scanned with a Typhoon FLA 9000 scanner (GE Healthcare). Data were analyzed using Multi Gauge V3.0 software (FujiFilm).

Analysis of mitochondrial mRNA half-life

Mitochondrial RNA stability was measured by metabolic labeling with 4-thiouridine, as previously described.[43] With this method we were able to tag the newly synthesized RNA, and separate it from the preexisting RNA. The half-life of a transcript is calculated based on the ratio of its preexisting fraction to its total amount. Incorporation of 4sU (250 μM, Sigma) into the newly synthesized transcripts was carried out for 1 h at 37 °C and 5% CO_2. The culture medium was then rapidly aspirated and cells were lysed in TRI Reagent (Sigma Aldrich). Extraction with chloroform was performed and RNA was precipitated with 2-propanol. The pellets were dissolved in water and diluted to a concentration of 1 μg/μL. One hundred μg of RNA was biotinylated for 1.5 h at room temperature in a biotinylation buffer (10 mM Tris-HCl, pH 7.4, 1 mM EDTA) using EZ-Link HPDP-Biotin (0.2 mg/mL; Pierce). RNA extraction was then performed with chloroform/isoamyl alcohol (24:1) and the RNA was then precipitated using 2-propanol and 0.25 M NaCl. The pellets were dissolved in water and diluted to a concentration of 1 μg/μL. Then 50 μg of biotinylated RNA was denatured for 10 min at 65 °C, then rapidly cooled on ice and incubated for 15 min at room temperature with 50 μL of streptavidin-coupled Dynabeads (Thermo Scientific). Unbound RNA (preexisting fraction) was transferred to new tubes. In further quantitative analyses the total RNA fraction and the preexisting fraction were used. The northern technique was used to measure the levels of individual transcripts as described above. Each sample was run in duplicate on a 1% agarose gel containing formaldehyde (0.9%). For preparation of strand-specific [α-32P] UTP-labeled riboprobes, PCR products were used as templates covering the following mtDNA fragments: 3652–4029 (ND1), 15088–15499 (CytB), 7586–7900 (COX2) and 8631–8932 (ATP8/6). After hybridization, exposure to phosphorimager screens, and data collection with a Typhoon FLA 9000 scanner (GE Healthcare), the intensity of the obtained signals was quantified using Multi Gauge V3.0 software (FujiFilm). RNA half-lives were calculated from the following equation: $t_{1/2}$=-(t × ln2 / ln

(1-R)), where t is time (in hours) of RNA labeling with 4sU (1 h) and R is the ratio of the amount of preexisting RNA to the amount of total RNA.

Mitochondrial translation evaluation

For the mitochondrial translation evaluation, cells were seeded at a density of 1.7×10^6 in 6 mm Petri dish the day before the experiment. After 24 h, the medium was changed with methionine/cysteine-free DMEM with the addition of FBS and Glutamine 1 mM and cells were placed in it at 37 °C for 1 h. Then, emetine was added to the medium to a final concentration of 100 μg/mL and cells were further incubated at 37 °C for 10 min. EasyTag™ EXPRESS^{35}S Protein Labeling Mix was added to the medium to a final concentration of 200 μCi/mL and the labeling was performed at 37 °C for 1 h. Cells were then washed twice with PBS, collected and resuspended in lysis buffer [PBS, protease inhibitor cocktail, PMFS 200 mM, 0.1% DDM, Viscolase, 1% SDS], incubated on ice for 15 min and then centrifuged at 14,000*g* for 20 min. The supernatant was collected, protein content was quantified with the Bradford reagent, and protein extracts were separated on SDS-PAGE at 15%. Gels were dried, and digital autoradiography was used for gel analysis with a Typhoon FLA 9500 scanner (GE Healthcare), followed by use of ImageQuant software (GE Healthcare).

BN-PAGE and OXPHOS efficiency evaluation

To test OXPHOS complexes stability, 500 μg of mitochondria isolated from Scr, shRNA, and APE1^{WT} clones were lysed in 1X NativePAGE Sample Buffer (LifeTechnologies) with 6 mg/mg mitochondria of Digitonin (Calbiochem) in a final volume of 50 μL. Samples were incubated on ice for 15 min and then centrifuged at 20,000*g* and 4 °C for 30 min. The supernatant was transferred into a new tube, quantified with the Bradford reagent, and 45 μg were separated on BN-PAGE. NativePAGE 5% G-250 Sample Additive (LifeTechnologies) was added to each sample before electrophoresis, which was performed on the NativePAGE Novex Bis-Tris Gel System (LifeTechnologies) with 4–16% Bis-Tris gels, following manufacturer's instructions. After electrophoresis, gels were stained with Coomassie R-250 stain.

Oxygen consumption rate (OCR) and extracellular acidification rate (ECAR) were determined by direct measurement with a SeaHorse Extracellular Flux Analyzer XpE instrument (Seahorse Bioscience, Agilent Technologies). The day before the measurement, 6×10^4 cells were seeded in XF cell culture microplates in a volume of 100 μL and left under the hood for 1 h to let the cells adhere to the bottom of the plate. The total volume of the wells was then adjusted to 500 μL and cells were left in the incubator O/N at 37 °C and with 5% CO_2 pressure. The next day, cells were washed twice with PBS and incubated with XF assay medium supplemented with 10 mM glucose, 1 mM glutamine and 1 mM pyruvate (pH 7.4) and placed in an incubator at 37 °C without CO_2 for 1 h. OCR and ECAR for the mitochondrial stress test were determined following the manufacturer's instructions. Briefly, ports in the cartridge plate were loaded with 1 μM oligomycin, 1 μM FCCP and, finally, a mixture of 0.25 μM Rotenone and 0.25 μM Antimycin A. Real-time OCR was averaged and recorded three times during each conditional cycle. Then cells were collected, lysed, and total protein content was measured with the Bradford reagent to normalize the number of cells for each well. For the statistical analysis, all values were normalized for the control (Scr) clone.

Statistical analyses

If not otherwise specified, data reported represents the mean ± SD of three independent biological replicates. Statistical analyses on biological data were performed using the Microsoft Excel data analysis program for Student's *t*-test analysis. Differences were considered to be statistically significant at $p < 0.05$.

CRediT authorship contribution statement

Arianna Barchiesi: Data curation, Formal analysis, Investigation, Methodology, Writing - original draft. **Veronica Bazzani:** Investigation and Methodology, Writing - original draft. **Agata Jabczynska:** Investigation and Methodology. **Lukasz S. Borowski:** Investigation and Methodology. **Silke Oeljeklaus:** Investigation and Methodology. **Bettina Warscheid:** Data curation, Formal analysis, Funding acquisition. **Agnieszka Chacinska:** Data curation, Formal analysis. **Roman J. Szczesny:** Data curation, Formal analysis, Funding acquisition, Writing - original draft. **Carlo Vascotto:** Conceptualization, Project administration, Data curation, Formal analysis, Funding acquisition, Writing - original draft, Writing - review & editing. Final approval of manuscript: All authors read and approved the final manuscript. Accountable for all aspects of the work: CV.

Acknowledgements

We thank Prof. Andrzej Dziembowski and Dr. Michal Wasilewski for helpful discussion and advice. We thank Anna Kotrys for comments on mitochondrial translation assay.

Funding

This work was supported by grants to CV from the Associazione Italiana per la Ricerca sul Cancro (MFAG 16780) and by the National Science Centre, Poland via POLONEZ grant agreement 2016/23/P/NZ1/03899, which has received funding from the European Union's Horizon 2020 research and innovation programme under the Marie Skłodowska-Curie grant agreement No 665778. The work of RJS was supported by the National Science Centre in Poland (UMO-2014/12/W/NZ1/00463). The work of BW was supported by the European Research Council (ERC) Consolidator Grant No. 648235, the Deutsche Forschungsgemeinschaft (DFG, German Research Foundation) Project ID 403222702/SFB 1381, and Germany's Excellence Strategy (CIBSS – EXC-2189 – Project ID 390939984).

Declaration of Competing Interest

The authors declare that they have no known competing financial interests or personal relationships that could have appeared to influence the work reported in this paper

Appendix A. Supplementary material

Supplementary data to this article can be found online at https://doi.org/10.1016/j.jmb.2021.167125.

Received 21 May 2021;
Accepted 26 June 2021;
Available online 2 July 2021

Keywords:
mitochondria;
apurinic/apyrimidinic endonuclease 1;
RNA processing;
oxidative phosphorylation

Abbreviations used:
AMA, antimycin A; APE1, apurinic/apyrimidinic endonuclease 1; BER, base excision repair; BrU, bromouridine; ECAR, extracellular acidification rate; IMS, intermembrane space; MCE, mitochondrial extract; MIA, mitochondrial IMS assembly; NLS, nuclear localization sequence; MTS, mitochondrial targeting signal; mtDNA, mitochondrial DNA; mtRNA, mitochondrial RNA; mt-mRNA, mitochondrial messenger RNA; MRGs, mitochondrial RNA granules; PLA, proximity ligation assay; ROS, reactive oxygen species; TCE, total cell extract; 4sU, 4-thiouridine

References

1. Demple, B., Herman, T., Chen, D.S., (1991). Cloning and expression of APE, the cDNA encoding the major human apurinic endonuclease: definition of a family of DNA repair enzymes. *Proc. Natl. Acad. Sci.*, **88**, 11450–11454. https://doi.org/10.1073/pnas.88.24.11450.
2. Xanthoudakis, S., Curran, T., (1992). Identification and characterization of Ref-1, a nuclear protein that facilitates AP-1 DNA-binding activity. *EMBO J.*, **11**, 653–665. https://doi.org/10.1002/j.1460-2075.1992.tb05097.x.
3. Xanthoudakis, S., Miao, G., Wang, F., Pan, Y.C., Curran, T., (1992). Redox activation of Fos-Jun DNA binding activity is mediated by a DNA repair enzyme. *EMBO J.*, **11**, 3323–3335.
4. Jayaraman, L., Murthy, K.G.K., Zhu, C., Curran, T., Xanthoudakis, S., Prives, C., (1997). Identification of redox/repair protein Ref-1 as a potent activator of p53. *Genes Dev.*, **11**, 558–570. https://doi.org/10.1101/gad.11.5.558.
5. Huang, L.E., Arany, Z., Livingston, D.M., Franklin Bunn, H., (1996). Activation of hypoxia-inducible transcription factor depends primarily upon redox-sensitive stabilization of its α subunit. *J. Biol. Chem.*, **271**, 32253–32259. https://doi.org/10.1074/jbc.271.50.32253.
6. Cardoso, A.A., Jiang, Y., Luo, M., Reed, A.M., Shahda, S., He, Y., Maitra, A., Kelley, M.R., et al., (2012). APE1/Ref-1 regulates STAT3 transcriptional activity and APE1/Ref-1-STAT3 Dual-targeting effectively inhibits pancreatic cancer cell survival. *PLoS One,*. https://doi.org/10.1371/journal.pone.0047462.
7. Huang, R.P., Adamson, E.D., (1993). Characterization of the DNA-binding properties of the early growth response-1 (Egr-1) transcription factor: evidence for modulation by a redox mechanism. *DNA Cell Biol.,*. https://doi.org/10.1089/dna.1993.12.265.
8. Cao, X., Kambe, F., Ohmori, S., Seo, H., (2002). Oxidoreductive modification of two cysteine residues in paired domain by Ref-1 regulates DNA-binding activity of Pax-8. *Biochem. Biophys. Res. Commun.,*. https://doi.org/10.1016/S0006-291X(02)02196-4.
9. Kim, Y.-J., Wilson III, D.M., (2012). Overview of base excision repair biochemistry. *Curr. Mol. Pharmacol.*, **5**, 3–13. https://doi.org/10.2174/1874467211205010003.
10. Chen, D.S., Herman, T., Demple, B., (1991). Two distinct human DNA diesterases that hydrolyze 3′-blocking deoxyribose fragments from oxidized DNA. *Nucleic Acids Res.*, **19**, 5907–5914. https://doi.org/10.1093/nar/19.21.5907.
11. Wilson, D.M., Takeshita, M., Grollman, A.P., Demple, B., (1995). Incision activity of human apurinic endonuclease (Ape) at abasic site analogs in DNA. *J. Biol. Chem.*, **270**, 16002–16007. https://doi.org/10.1074/jbc.270.27.16002.
12. Vohhodina, J., Harkin, D.P., Savage, K.I., (2016). Dual roles of DNA repair enzymes in RNA biology/post-transcriptional control. *Wiley Interdiscip. Rev. RNA*, **7**, 604–619. https://doi.org/10.1002/wrna.1353.
13. Barzilay, G., Walker, L.J., Robson, C.N., Hickson, I.D., (1995). Site-directed mutagenesis of the human DNA repair enzyme HAP1: Identification of residues important for AP endonuclease and RNase H activity. *Nucleic Acids Res.*, **23**, 1544–1550. https://doi.org/10.1093/nar/23.9.1544.
14. Berquist, B.R., McNeill, D.R., Wilson, D.M., (2008). Characterization of Abasic endonuclease activity of human Ape1 on alternative substrates, as well as effects of ATP and sequence context on AP site incision. *J. Mol. Biol.*, **379**, 17–27. https://doi.org/10.1016/j.jmb.2008.03.053.

15. Barnes, T., Kim, W.C., Mantha, A.K., Kim, S.E., Izumi, T., Mitra, S., Lee, C.H., (2009). Identification of Apurinic/apyrimidinic endonuclease 1 (APE1) as the endoribonuclease that cleaves c-myc mRNA. *Nucleic Acids Res.*, **37**, 3946–3958. https://doi.org/10.1093/nar/gkp275.
16. Vascotto, C., Fantini, D., Romanello, M., Cesaratto, L., Deganuto, M., Leonardi, A., Radicella, J.P., Kelley, M.R., et al., (2009). APE1/Ref-1 interacts with NPM1 within nucleoli and plays a role in the rRNA quality control process. *Mol. Cell. Biol.*, **29**, 1834–1854. https://doi.org/10.1128/MCB.01337-08.
17. Malfatti, M.C., Balachander, S., Antoniali, G., Koh, K.D., Saint-Pierre, C., Gasparutto, D., Chon, H., Crouch, R.J., et al., (2017). Abasic and oxidized ribonucleotides embedded in DNA are processed by human APE1 and not by RNase H2. *Nucleic Acids Res.*, **403**, 451–456. https://doi.org/10.1093/nar/gkx723.
18. Antoniali, G., Serra, F., Lirussi, L., Tanaka, M., D'Ambrosio, C., Zhang, S., Radovic, S., Dalla, E., et al., (2017). Mammalian APE1 controls miRNA processing and its interactome is linked to cancer RNA metabolism. *Nature Commun.*, **8** https://doi.org/10.1038/s41467-017-00842-8.
19. Li, M., Zhong, Z., Zhu, J., Xiang, D., Dai, N., Cao, X., Qing, Y., Yang, Z., et al., (2010). Identification and characterization of mitochondrial targeting sequence of human apurinic/apyrimidinic endonuclease. *J. Biol. Chem.*, **285**, 14871–14881. https://doi.org/10.1074/jbc.M109.069591.
20. Barchiesi, A., Wasilewski, M., Chacinska, A., Tell, G., Vascotto, C., (2015). Mitochondrial translocation of APE1 relies on the MIA pathway. *Nucleic Acids Res.*, **43**, 5451–5464. https://doi.org/10.1093/nar/gkv433.
21. Barchiesi, A., Bazzani, V., Tolotto, V., Elancheliyan, P., Wasilewski, M., Chacinska, A., Vascotto, C., (2020). Mitochondrial oxidative stress induces rapid intermembrane space/matrix translocation of apurinic/apyrimidinic endonuclease 1 protein through TIM23 complex. *J. Mol. Biol.*,. https://doi.org/10.1016/j.jmb.2020.11.012.
22. Grishko, V.I., Rachek, L.I., Spitz, D.R., Wilson, G.L., LeDoux, S.P., (2005). Contribution of mitochondrial DNA repair to cell resistance from oxidative stress. *J. Biol. Chem.*,. https://doi.org/10.1074/jbc.M413022200.
23. Hanahan, D., Weinberg, R.A., (2011). Hallmarks of cancer: the next generation. *Cell*, **144**, 646–674. https://doi.org/10.1016/j.cell.2011.02.013.
24. Nakabeppu, Y., (2014). Cellular levels of 8-oxoguanine in either DNA or the nucleotide pool play pivotal roles in carcinogenesis and survival of cancer cells. *Int. J. Mol. Sci.*, **15**, 12543–12557. https://doi.org/10.3390/ijms150712543.
25. Copeland, W.C., Longley, M.J., (2014). Mitochondrial genome maintenance in health and disease. *DNA Repair (Amst).*, **19**, 190–198. https://doi.org/10.1016/j.dnarep.2014.03.010.
26. Fleming, A.M., Alshykhly, O., Zhu, J., Muller, J.G., Burrows, C.J., (2015). Rates of chemical cleavage of DNA and RNA oligomers containing guanine oxidation products. *Chem. Res. Toxicol.*, **28**, 1292–1300. https://doi.org/10.1021/acs.chemrestox.5b00096.
27. Fimognari, C., (2015). Role of oxidative RNA damage in chronic-degenerative diseases. *Oxid. Med. Cell. Longev.*, **2015** https://doi.org/10.1155/2015/358713.
28. Shan, X., Lin, C.G., (2006). Quantification of oxidized RNAs in Alzheimer's disease. *Neurobiol. Aging*, **27**, 657–662. https://doi.org/10.1016/j.neurobiolaging.2005.03.022.
29. Ding, Q., (2005). Ribosome dysfunction is an early event in Alzheimer's disease. *J. Neurosci.*, **25**, 9171–9175. https://doi.org/10.1523/JNEUROSCI.3040-05.2005.
30. Szczesny, R.J., Borowski, L.S., Brzezniak, L.K., Dmochowska, A., Gewartowski, K., Bartnik, E., Stepien, P.P., (2009). Human mitochondrial RNA turnover caught in flagranti: involvement of hSuv3p helicase in RNA surveillance. *Nucleic Acids Res.*, **38**, 279–298. https://doi.org/10.1093/nar/gkp903.
31. Borowski, L.S., Dziembowski, A., Hejnowicz, M.S., Stepien, P.P., Szczesny, R.J., (2013). Human mitochondrial RNA decay mediated by PNPase-hSuv3 complex takes place in distinct foci. *Nucleic Acids Res.*, **41**, 1223–1240. https://doi.org/10.1093/nar/gks1130.
32. Levy, S., Allerston, C.K., Liveanu, V., Habib, M.R., Gileadi, O., Schuster, G., (2016). Identification of LACTB2, a metallo-β-lactamase protein, as a human mitochondrial endoribonuclease. *Nucleic Acids Res.*, **44**, 1813–1832. https://doi.org/10.1093/nar/gkw050.
33. Vascotto, C., Bisetto, E., Li, M., Zeef, L.A.H., D'Ambrosio, C., Domenis, R., Comelli, M., Delneri, D., et al., (2011). Knock-in reconstitution studies reveal an unexpected role of Cys-65 in regulating APE1/Ref-1 subcellular trafficking and function. *Mol. Biol. Cell.*, **22**, 3887–3901. https://doi.org/10.1091/mbc.E11-05-0391.
34. Vascotto, C., Cesaratto, L., Zeef, L.A.H., Deganuto, M., D'Ambrosio, C., Scaloni, A., Romanello, M., Damante, G., et al., (2009). Genome-wide analysis and proteomic studies reveal APE1/Ref-1 multifunctional role in mammalian cells. *Proteomics*, **9**, 1058–1074. https://doi.org/10.1002/pmic.200800638.
35. Mantha, A.K., Sarkar, B., Tell, G., (2014). A short review on the implications of base excision repair pathway for neurons: relevance to neurodegenerative diseases. *Mitochondrion*, **16**, 38–49. https://doi.org/10.1016/j.mito.2013.10.007.
36. Tanaka, M., Jaruga, P., Küpfer, P.A., Leumann, C.J., Dizdaroglu, M., Sonntag, W.E., Boon Chock, P., (2012). RNA oxidation catalyzed by cytochrome c leads to its depurination and cross-linking, which may facilitate cytochrome c release from mitochondria. *Free Radic. Biol. Med.*, **53**, 854–862. https://doi.org/10.1016/j.freeradbiomed.2012.05.044.
37. Quinlan, C.L., Gerencser, A.A., Treberg, J.R., Brand, M.D., (2011). The mechanism of superoxide production by the antimycin-inhibited mitochondrial Q-cycle. *J. Biol. Chem.*, **286**, 31361–31372. https://doi.org/10.1074/jbc.M111.267898.
38. Petruk, S., Fenstermaker, T.K., Black, K.L., Brock, H.W., Mazo, A., (2016). Detection of RNA-DNA association by a proximity ligation-based method. *Sci. Rep.*, **6** https://doi.org/10.1038/srep27313.
39. Söderberg, O., Gullberg, M., Jarvius, M., Ridderstråle, K., Leuchowius, K.J., Jarvius, J., Wester, K., Hydbring, P., et al., (2006). Direct observation of individual endogenous protein complexes in situ by proximity ligation. *Nature Methods*, **3**, 995–1000. https://doi.org/10.1038/nmeth947.
40. Jackson, E.B., Theriot, C.A., Chattopadhyay, R., Mitra, S., Izumi, T., (2005). Analysis of nuclear transport signals in the human apurinic/apyrimidinic endonuclease (APE1/

Ref1). *Nucleic Acids Res.*, **33**, 3303–3312. https://doi.org/10.1093/nar/gki641.
41. Bazzani, V., Barchiesi, A., Radecka, D., Pravisani, R., Guadagno, A., Di Loreto, C., Baccarani, U., Vascotto, C., (2020). Mitochondrial apurinic/apyrimidinic endonuclease 1 enhances mtDNA repair contributing to cell proliferation and mitochondrial integrity in early stages of hepatocellular carcinoma. *BMC Cancer*, **20** https://doi.org/10.1186/s12885-020-07258-6.
42. Rai, G., Vyjayanti, V.N., Dorjsuren, D., Simeonov, A., Jadhav, A., Wilson, D.M., Maloney, D.J., (2012). Synthesis, biological evaluation, and structure-activity relationships of a novel class of apurinic/apyrimidinic endonuclease 1 inhibitors. *J. Med. Chem.*,. https://doi.org/10.1021/jm201537d.
43. Borowski, L.S., Szczesny, R.J., (2014). Measurement of mitochondrial RNA stability by metabolic labeling of transcripts with 4-thiouridine. *Methods Mol. Biol.*, **1125**, 277–286. https://doi.org/10.1007/978-1-62703-971-0_22.
44. McKee, E.E., Ferguson, M., Bentley, A.T., Marks, T.A., (2006). Inhibition of mammalian mitochondrial protein synthesis by oxazolidinones. *Antimicrob. Agents Chemother.*, **50**, 2042–2049. https://doi.org/10.1128/AAC.01411-05.
45. Signes, A., Fernandez-Vizarra, E., (2018). Assembly of mammalian oxidative phosphorylation complexes I-V and supercomplexes. *Essays Biochem.*, **62**, 255–270. https://doi.org/10.1042/EBC20170098.
46. Acín-Pérez, R., Bayona-Bafaluy, M.P., Fernández-Silva, P., Moreno-Loshuertos, R., Pérez-Martos, A., Bruno, C., Moraes, C.T., Enríquez, J.A., (2004). Respiratory complex III is required to maintain complex I in mammalian mitochondria. *Mol. Cell.*, **13**, 805–815. https://doi.org/10.1016/S1097-2765(04)00124-8.
47. Li, Y., D'Aurelio, M., Deng, J.H., Park, J.S., Manfredi, G., Hu, P., Lu, J., Bai, Y., (2007). An assembled complex IV maintains the stability and activity of complex I in mammalian mitochondria. *J. Biol. Chem.*, **282**, 17557–17562. https://doi.org/10.1074/jbc.M701056200.
48. Cortés-Hernández, P., Vázquez-Memije, M.E., García, J. J., (2007). ATP6 homoplasmic mutations inhibit and destabilize the human F 1F0-ATP synthase without preventing enzyme assembly and oligomerization. *J. Biol. Chem.*, **282**, 1051–1058. https://doi.org/10.1074/jbc.M606828200.
49. Divakaruni, A.S., Paradyse, A., Ferrick, D.A., Murphy, A. N., Jastroch, M., (2014). Analysis and interpretation of microplate-based oxygen consumption and pH data. *Methods Enzymol.*,. https://doi.org/10.1016/B978-0-12-801415-8.00016-3.
50. Dott, W., Mistry, P., Wright, J., Cain, K., Herbert, K.E., (2014). Modulation of mitochondrial bioenergetics in a skeletal muscle cell line model of mitochondrial toxicity. *Redox Biol.*,. https://doi.org/10.1016/j.redox.2013.12.028.
51. Shah, F., Logsdon, D., Messmann, R.A., Fehrenbacher, J. C., Fishel, M.L., Kelley, M.R., (2017). Exploiting the Ref-1-APE1 node in cancer signaling and other diseases: from bench to clinic. *Npj Precis. Oncol.*, **1**, 19. https://doi.org/10.1038/s41698-017-0023-0.
52. Chattopadhyay, R., Wiederhold, L., Szczesny, B., Boldogh, I., Hazra, T.K., Izumi, T., Mitra, S., (2006). Identification and characterization of mitochondrial abasic (AP)-endonuclease in mammalian cells. *Nucleic Acids Res.*, **34**, 2067–2076. https://doi.org/10.1093/nar/gkl177.
53. Kang, M.W., Kang, S.K., Choi, S., Lee, C.S., Jeon, B.H., Lim, S.P., (2012). Upregulation of APE/ref-1 in recurrence stage I, non small cell lung cancer. *Asian Cardiovasc. Thorac. Ann.*, **20**, 36–41. https://doi.org/10.1177/0218492311432800.
54. Di Maso, V., Avellini, C., Crocè, L.S., Rosso, N., Quadrifoglio, F., Cesaratto, L., Codarin, E., Bedogni, G., et al., (2006). Subcellular localization of APE1/Ref-1 in human hepatocellular carcinoma: possible prognostic significance. *Mol. Med.*, **13**, 30–39. https://doi.org/10.2119/2006.
55. Kim, J.S., Kim, J.M., Liang, Z.L., Jang, J.Y., Kim, S., Huh, G.J., Kim, K.H., Cho, M.J., (2012). Prognostic significance of human apurinic/apyrimidinic endonuclease (APE/Ref-1) expression in rectal cancer treated with preoperative radiochemotherapy. *Int. J. Radiat. Oncol. Biol. Phys.*, **82**, 130–137. https://doi.org/10.1016/j.ijrobp.2010.09.037.
56. Frehlick, L.J., Eirín-López, J.M., Ausió, J., (2007). New insights into the nucleophosmin/nucleoplasmin family of nuclear chaperones. *BioEssays.*, **29**, 49–59. https://doi.org/10.1002/bies.20512.
57. Siddiqui, A., Rivera-Sánchez, S., Castro, M.D.R., Acevedo-Torres, K., Rane, A., Torres-Ramos, C.A., Nicholls, D.G., Andersen, J.K., et al., (2012). Mitochondrial DNA damage is associated with reduced mitochondrial bioenergetics in Huntington's disease. *Free Radic. Biol. Med.*, **53**, 1478–1488. https://doi.org/10.1016/j.freeradbiomed.2012.06.008.
58. Joo, H.K., Lee, Y.R., Park, M.S., Choi, S., Park, K., Lee, S. K., Kim, C.S., Park, J.B., Jeon, B.H., (2014). Mitochondrial APE1/Ref-1 suppressed protein kinase C-induced mitochondrial dysfunction in mouse endothelial cells. *Mitochondrion*, **17**, 42–49. https://doi.org/10.1016/j.mito.2014.05.006.
59. Torregrosa-Muñumer, R., Gómez, A., Vara, E., Kireev, R., Barja, G., Tresguerres, J.A.F., Gredilla, R., (2016). Reduced apurinic/apyrimidinic endonuclease 1 activity and increased DNA damage in mitochondria are related to enhanced apoptosis and inflammation in the brain of senescence- accelerated P8 mice (SAMP8). *Biogerontology*, **17**, 325–335. https://doi.org/10.1007/s10522-015-9612-x.
60. Greim, H., Albertini, R.J., (2014). Cellular response to the genotoxic insult: The question of threshold for genotoxic carcinogens. *Toxicol. Res. (Camb).*,. https://doi.org/10.1039/c4tx00078a.
61. Friedman, J.I., Stivers, J.T., (2010). Detection of damaged DNA bases by DNA glycosylase enzymes. *Biochemistry*,. https://doi.org/10.1021/bi100593a.
62. Lirussi, L., Demir, Ö., You, P., Sarno, A., Amaro, R.E., Nilsen, H., (2021). RNA metabolism guided by RNA modifications: the role of SMUG1 in rRNA quality control. *Biomolecules*,. https://doi.org/10.3390/biom11010076.
63. Prakash, A., Doublié, S., (2015). Base excision repair in the mitochondria. *J. Cell. Biochem.*, **116**, 1490–1499. https://doi.org/10.1002/jcb.25103.
64. Cameron, T.A., Matz, L.M., De Lay, N.R., (2018). Polynucleotide phosphorylase: Not merely an RNase but a pivotal post-transcriptional regulator. *PLoS Genet.*, **14**, https://doi.org/10.1371/journal.pgen.1007654 e1007654.
65. Wang, D.D.H., Shu, Z., Lieser, S.A., Chen, P.L., Lee, W.H., (2009). Human mitochondrial SUV3 and polynucleotide phosphorylase form a 330-kDa heteropentamer to cooperatively degradedouble-stranded RNA with a 3′-to-

5′ directionality. *J. Biol. Chem.*, **284**, 20812–20821. https://doi.org/10.1074/jbc.M109.009605.

66. Szczesny, R.J., Obriot, H., Paczkowska, A., Jedrzejczak, R., Dmochowska, A., Bartnik, E., Formstecher, P., Polakowska, R., et al., (2007). Down-regulation of human RNA/DNA helicase SUV3 induces apoptosis by a caspase- and AIF-dependent pathway. *Biol. Cell.*, **99**, 323–332. https://doi.org/10.1042/BC20060108.
67. Chen, H.-W., Rainey, R.N., Balatoni, C.E., Dawson, D.W., Troke, J.J., Wasiak, S., Hong, J.S., McBride, H.M., et al., (2006). Mammalian polynucleotide phosphorylase is an intermembrane space RNase that maintains mitochondrial homeostasis. *Mol. Cell. Biol.*, **26**, 8475–8487. https://doi.org/10.1128/MCB.01002-06.
68. Bustin, S.A., Benes, V., Garson, J.A., Hellemans, J., Huggett, J., Kubista, M., Mueller, R., Nolan, T., et al., (2009). The MIQE guidelines: minimum information for publication of quantitative real-time PCR experiments. *Clin. Chem.*,. https://doi.org/10.1373/clinchem.2008.112797.
69. Tanaka, M., Han, S., Küpfer, P.A., Leumann, C.J., Sonntag, W.E., (2011). Quantification of oxidized levels of specific RNA species using an Aldehyde Reactive Probe. *Anal. Biochem.*, **417**, 142–148. https://doi.org/10.1016/j.ab.2011.05.038.